

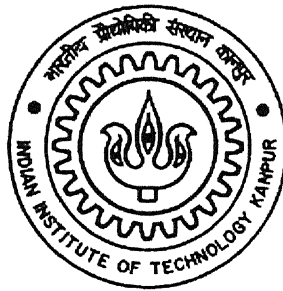
**CHARACTERIZATION OF PRESSURE AND SHEAR
WAVES IN ALUMINUM USING LASER BASED
ULTRASONIC SYSTEM**

A thesis Submitted
in partial Fulfillment of the Requirements
for the Degree of

MASTER OF TECHNOLOGY

By

S.SOLOMON RAJ



to the
**DEPARTMENT OF MECHANICAL ENGINEERING
INDIAN INSTITUTE OF TECHNOLOGY, KANPUR
AUGUST 2004.**

TH
ME/2004/m
R137c

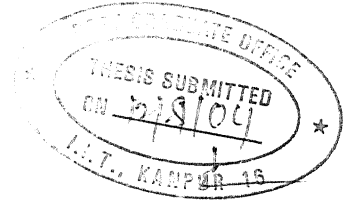
21 OCT 2004

बुद्धोत्तम काशीनाथ केलकर पुस्तकालय
भारतीय प्रौद्योगिकी संस्थान कानपुर
अवधि क्र० A...149261.....



A149261

CERTIFICATE



It is certified that the work contained in the thesis entitled "**CHARACTERIZATION OF PRESSURE AND SHEAR WAVES IN ALUMINUM USING LASER BASED ULTRASONIC SYSTEM**" by **Mr. Solomon Raj** has been carried out under our supervision and this work has not been submitted elsewhere for a degree.

(Dr. V. Raghuram)

Department of Mechanical Engineering
Indian Institute of Technology, Kanpur.

(Dr. N. N. Kishore)

Department of Mechanical Engineering
Indian Institute of Technology, Kanpur.

August, 2004

**DEDICATED
TO
MY BELOVED PARENTS**

ACKNOWLEDGEMENTS

At the beginning, I would like to thank and express my deepest regards and most sincere gratitude to my instructors and thesis supervisors Dr. N. N. Kishore and Dr .V. Raghuram for their sincere involvement, active guidance and moral support through out this work. Their inspiration and support made my work successful.

I wish to express my heartfelt thanks to Dr. Mrs. V. Raghuram for being pivotal, with her invaluable suggestions and constant encouragement towards the completion of this work.

I wish to thank especially the families of Dr. Joseph John, Dr. Sundarmanoharan and Mr.Shibu clement for their constant support, love and encouragement, which made my stay at IITK, enjoyable and memorable one. I do miss them a lot when I go out of IIT campus.

I appreciate and extend my thanks to laboratory mates Patil, Ankit, Bhanu, Mukul ji and Arvind ji for being so cooperative and encouraging.

My special thanks to Naveen, and Dhruv who helped me as far as programming part is concerned.

I am very much thankful to Shri S.K.Trivedi, who prepared all the test samples and fixtures in a very short time and professionally.

I do remember with reverence the encouragement and a moral support from my parents, sisters and brother, who always remain behind the scene, but stood by me providing inspiration through out this work, without which I would not have reached this stage.

S. Solomon Raj

ABSTRACT

Ultrasound generated in materials with laser irradiation is an important technique to carry out NDT of components. One advantage of laser ultrasonics is that it is contact-free, which can be employed for investigations of hot, fast moving or complicated shaped samples. In the present study, Nd-YAG pulsed laser is used for generation of ultrasound in samples in ablation regime and a He-Ne optical heterodyne interferometer is used for the detection of ultrasound. The pressure and shear wave generation and detection are characterized in aluminum cylindrical and rectangular samples in ablation regime. The simplicity of the experimental configuration adopted in the present studies brings out the scope of the applicability of existing Laser Based Ultrasonic (LBU) system. The wave data is analyzed using Short Time Fourier Transform (STFT) method and a method is proposed to differentiate S-wave and P-wave components. Using this procedure:

1. The pressure wave and shear wave has been characterized.
2. The radiation pattern of laser source for both pressure and shear wave is obtained in ablation regime.

CONTENTS

CERTIFICATE		ii
ACKNOWLEDGEMENTS		iv
ABSTRACT		v
LIST OF FIGURES		ix
 CHAPTER 1	 INTRODUCTION	 1
1.1	Introduction	1
1.2	NDT/NDE Methods	2
1.2.1	Visual and optical testing	
1.2.2	Penetrant testing	2
1.2.3	Magnetic testing	3
1.2.4	Electromagnetic or eddy current testing	3
1.2.5	Radiography	3
1.2.6	Acoustic emission testing	3
1.2.7	Leak testing	4
1.2.8	Ultrasonic testing	4
1.2.9	Laser ultrasonics	5
1.3	Literature survey	6
1.4	Present work	9
1.5	Thesis organization	10
 CHAPTER 2	 BASICS OF LASER ULTRASONICS	 11
2.1	Introduction	11
2.2	Main properties of laser light	12
2.2.1	Monochromaticity	12
2.2.2	Coherence	12
2.2.3	Directionality	13
2.2.4	High intensity or brightness	14
2.3	Basic principle of laser operation	15
2.4	Lasers for ultrasound generation	16
2.5	Lasers for interferometry	17
2.6	Laser-irradiated ultrasound modes	18
2.6.1	The thermoelastic regime	18
2.6.2	The constrained surface regime	18
2.6.3	The plasma (ablation) regime	19
2.7	Principle of laser interferometry	19

2.8	He-Ne laser Heterodyne interferometer	20
2.8.1	Working of heterodyne interferometer (optics)	20
2.8.2	Principle of detection	21
2.8.3	Sensitivity	22
2.9	Types of ultrasonic waves	22
2.9.1	Longitudinal waves	23
2.9.2	Transverse waves	23
2.10	Closure	23
CHAPTER 3	EXPERIMENTAL SET-UP AND PROCEDURE	29
3.1	Experimental Set-up (LBU)	29
3.1.1	Nd: YAG pulsed laser ultrasonic generator	29
3.1.2	Optical heterodyne laser (He-Ne) probe	30
3.1.3	Digital storage oscilloscope	30
3.2	Experimental procedure (LBU)	31
3.2.1	Calibration of set-up	31
3.2.2	Scanning procedure	31
3.3	Closure	32
CHAPTER 4	RADIATION PATTERN AND SIGNAL PROCESSING	36
4.1	Radiation patterns for laser ultrasonic sources	36
4.1.1	Ablation source	36
4.2	Signal processing	38
4.2.1	Digitizing the time axis	39
4.2.2	Digitizing signal amplitude	39
4.2.3	Time - frequency analysis	40
4.2.4	Time and frequency	40
4.2.5	Short-time Fourier transform (STFT)	40
4.2.6	Spectrogram	40
4.3	Closure	42
CHAPTER 5	RESULTS AND DISCUSSION	43
5.1	Experimental details	43
5.2	Directivity pattern of laser source for pressure wave	44
5.2.1	Sample of 25mm radius	45
5.2.2	Sample of 20mm radius	49
5.2.3	Sample of 40mm radius	51
5.3	Shear wave identification	53
5.4	Shear wave time of arrival and its directivity in a 25mm	56
5.4.1	Time of arrival of shear wave	57
5.4.2	Shear wave directivity pattern	60

CHAPTER 6	CONCLUSIONS AND SCOPE FOR FUTURE WORK	62
6.1	Conclusions	62
6.2	Scope for future work	62
REFERENCES		64
Appendix A		67
Appendix B		68

List of Figures

2.1 Comparison of ordinary light and laser light	24
2.2 Simplified energy level diagram for a laser medium	24
2.3 Thermoelastic regime	24
2.4 (a-d) Schematic diagram showing stresses induced when a laser pulse is incident on a sample	25
2.5 Schematic diagram to show ablation of surface material and net reactive force on sample	27
2.6 Optical layout of heterodyne interferometer	28
3.1 Schematic layout of experimental setup (LBU)	33
3.2 (a-b) Photograph of experimental setup (LBU)	34
4.1 Theoretical directivity pattern of pressure wave in aluminum	37
4.2 Theoretical directivity pattern of shear wave in aluminum	38
5.1 Epi-central measurement	43
5.2 Off- epicentral measurement with shear displacements	44
5.3 Semi cylindrical sample with pulsed laser and heterodyne interferometer	45
5.4 Signal collected in 25mm radius sample at 10^0 from the epicenter	45
5.5 Signal collected in 25mm radius sample at 20^0 from epicenter	46
5.6 Signal collected in 25mm radius sample at 30^0 from epicenter	46
5.7 Signal collected in 25mm radius sample at 40^0 from epicenter	47
5.8 Signal collected in 25mm radius sample at 50^0 from epicenter	47
5.9 Signal collected in 25mm radius sample at 60^0 from epicenter	48
5.10 Experimentally obtained directivity of pressure wave in 25mm radius	48
5.11 Signal collected in 20mm radius sample at 0^0 from epicenter	49
5.12 Signal collected in 20mm radius sample at 30^0 from epicenter	50
5.13 Signal collected in 20mm radius sample at 50^0 from epicenter	50
5.14 Directivity of pressure wave at 20mm radius	51
5.15 Signal collected in 40mm radius sample at 10^0 from epicenter	51

5.16 Signal in collected in 40mm radius sample at 20^0 from epicenter	52
5.17 Signal collected in 40mm radius sample at 50^0 from epicenter	52
5.18 Experimentally obtained directivity of pressure wave in 40mm radius	53
5.19 Rectangular sample	54
5.20 Combined FFT of signals collected at 0^0 and 45^0	55
5.21 Stepped sample	56
5.22 FFT plots of the signals collected at various angles	57
5.23 (a) Time-frequency plot of signal at 30^0 from epicenter	58
5.23 (b) Time-frequency plot of signal at 40^0 from epicenter	58
5.23 (c) Time-frequency plot of signal at 50^0 from epicenter	59
5.23 (d) Time-frequency plot of signal at 60^0 from epicenter	59
5.23 (e) Time-frequency plot of signal at 70^0 from epicenter	60
5.24 Directivity of shear wave	61

Chapter 1

INTRODUCTION

1.1 INTRODUCTION

Non-destructive testing (NDT) may be defined as the application of an inspection method to a component or structure in which the test piece is not adversely affected by the testing method. Generally, NDT is normally carried out in one of the following circumstances:

1. As a control check and an aid to the monitoring of quality during manufacture. In this case NDT is used to check the maintenance of required quality levels during manufacture. The presence of manufacturing imperfections and defects may be detected. The physical characteristics and the severity of such imperfections and defects may also be assessed.
2. During in-service inspection. In this case NDT methods are used in order to detect any physical deterioration in a component or structure that might occur under service conditions. NDT methods are most usually employed to detect cracking, or crack propagation from existing defects. Such cracking is commonly associated with some form of fatigue.
3. Critical defect assessment. This use of NDT normally involves an in-depth examination of known defects in a structure in order to provide detailed information for "fitness for purpose" assessments and fracture mechanics calculations.

The field of Nondestructive Testing (NDT) is a very broad, interdisciplinary field that plays a critical role in assuring that structural components and systems perform their function in a reliable and cost effective fashion. NDT technicians and engineers define and implement tests that locate and characterize material conditions and flaws that might otherwise cause planes to crash, reactors to fail, pipelines to burst, and a variety of less visible, but equally troubling events. These tests are performed in a manner that does not affect the future usefulness of the object or material. In other words, NDT allows parts and materials to be inspected and measured without damaging them. Because it allows inspection without interfering with a product's final use, NDT provides an excellent

balance between quality control and cost-effectiveness. Generally speaking, NDT applies to industrial inspections. While technologies that are used in NDT are similar to those used in the medical industry, typically nonliving objects are the subjects of the inspections.

Nondestructive Evaluation (NDE) is a term that is often used interchangeably with NDT. However, technically, NDE is used to describe measurements that are more quantitative in nature. For example, a NDE method would not only locate a defect, but it would also be used to measure something about that defect such as its size, shape, and orientation. NDE may be used to determine material properties such as fracture toughness, formability, and other physical characteristics.

1.2 NDT/NDE Methods

The number of NDT methods that can be used to inspect components and make measurements is large and continues to grow. Researchers continue to find new ways of applying physics and other scientific disciplines to develop better NDT methods. However, there are few NDT methods that are used most often. These methods are visual inspection, penetrant testing, magnetic particle testing, electromagnetic or eddy current testing, radiography, and ultrasonic testing. These methods and a few others are briefly described below.

1.2.1 Visual and Optical Testing

Visual inspection involves using an inspector's eyes to look for defects. The inspector may also use special tools such as magnifying glasses, mirrors, to gain access and more closely inspect the subject area. Visual examiners follow procedures that range from simple to very complex.

1.2.2 Penetrant Testing

Test objects are coated with visible or fluorescent dye solution. Excess dye is then removed from the surface, and a developer is applied. The developer acts as blotter, drawing trapped penetrant out of imperfections open to the surface. With visible dyes, vivid color contrasts between the penetrant and developer make "bleedout" easy to see.

With fluorescent dyes, ultraviolet light is used to make the bleedout fluoresce brightly, thus allowing imperfections to be readily seen.

1.2.3 Magnetic Testing

This NDE method is accomplished by inducing a magnetic field in a ferromagnetic material and then dusting the surface with iron particles (either dry or suspended in liquid). Surface and near-surface imperfections distort the magnetic field and concentrate iron particles near imperfections, providing a visual indication of the flaw.

1.2.4 Electromagnetic Testing or Eddy Current testing

Electrical currents are generated in a conductive material by an induced alternating magnetic field. The electrical currents are called eddy currents because they flow in circles at and just below the surface of the material. Interruptions in the flow of eddy currents, caused by imperfections, dimensional changes, or changes in the material's conductive and permeability properties, can be detected with the proper equipment.

1.2.5 Radiography (RT)

Radiography involves the use of penetrating gamma or X-radiation to examine parts and products for imperfections. An X-ray generator or radioactive isotope is used as a source of radiation. Radiation is directed through a part and onto film or other imaging media. The resulting shadowgraph shows the dimensional features of the part. Possible imperfections are indicated as density changes on the film in the same manner as a medical X-ray shows broken bones.

1.2.6 Acoustic Emission Testing (AE)

When a solid material is stressed, imperfections within the material emit short bursts of acoustic energy called "emissions." As in ultrasonic testing, acoustic emissions can be detected by special receivers. Emission sources can be evaluated through the study of their intensity, rate, and location.

1.2.7 Leak Testing

Several techniques are used to detect and locate leaks in pressure containment parts, pressure vessels, and structures. Leaks can be detected by using electronic listening devices, pressure gauge measurements, liquid and gas penetrant techniques, and/or a simple soap-bubble test.

1.2.8 Ultrasonic Testing (UT)

Ultrasonics use transmission of high-frequency sound waves into a material to detect imperfections or to locate changes in material properties. The most commonly used ultrasonic testing technique is pulse echo, wherein sound is introduced into a test object and reflections (echoes) are returned to a receiver from internal imperfections or from the part's geometrical surfaces. Ultrasonics is a powerful technique for inspecting and characterizing industrial materials. It can not only to detect bulk and surface flaws, but also obtain information on material microstructure, which determines engineering properties, such as elastic moduli and ultimate strength. However, traditional ultrasound requires liquid or contact coupling for its generation and detection, making it difficult or impossible to apply in many industrial situations. This occurs in particular on curved parts and on parts at elevated temperature, a situation widely found in industrial products and during the processing of industrial materials. The ultrasonic waves are usually produced by making a piezoelectric ceramic transducer to vibrate under an electrical impulse. The waves are then coupled to the object (or body) under inspection by using a liquid or viscous film to establish a contact between the emitting transducer and the object (or body). A common practice, particularly in the aeronautic industry, consists of immersing the object in a water bath or to use water jets. Usually, the emitting transducer is also used as receiver of the ultrasonic echoes, i. e. the waves reflected by acoustic discontinuities inside the inspected object (or body), and it produces electrical signals indicative of these discontinuities. These discontinuities could for example be, in the case of material inspection, a layer of a different material, a crack, a disbond, a delamination, etc. This technique, called more precisely pulse-echo ultrasonics, provides not only information on the existence of such discontinuities, but also an indication on their depth, which is deduced from the time arrival of the signal and the knowledge of the acoustic propagation velocity.

1.2.9 Laser Ultrasonics

The light beam produced by most lasers is pencil-sized, and maintains its size and direction over very large distances; this sharply focused beam of coherent light is suitable for a wide variety of applications. With laser-ultrasonics, generation and detection of the ultrasound can be made at a distance, without any physical contact with the surface of the component to be inspected. No coupling medium is required. Also, the ultrasonic probing pulse is emitted in a direction normal to the surface of the component following laser light absorption, regardless of the angle of incidence of the generated laser beam. There is no need for normal incidence to the surface as is required for conventional pulse-echo ultrasonic inspection systems. Hence, no particular knowledge of the component's shape is needed prior to the inspection. Hence Laser-based ultrasound generation and detection overcomes some of the shortcomings of the other NDE methods, and make truly non-contact ultrasonic measurements in both electrically conductive and non-conductive materials, in materials at elevated temperatures, in corrosive and other hostile environments, in geometrically difficult to reach locations, and do all of these at relatively large distances from the test object surface. Furthermore, lasers are able to produce simultaneously shear and longitudinal bulk wave modes, as well as Rayleigh and Lamb wave modes. LBU system uses a pulsed laser to generate ultrasound and a continuous wave (CW) optical heterodyne interferometer to detect the ultrasound at the point of examination to perform ultrasonic inspection. An additional benefit of laser techniques is that they are capable of a high degree of absolute accuracy, since measurements can in principle be calibrated against the wavelength of light. There may be sensitivity penalties for using lasers rather than piezoelectric transducers or probes, and certainly they are likely to be more costly and complex to use. Nevertheless they are beginning to make a small but significant impact in a limited number of applications where their benefits over other probes outweigh their disadvantages.

Inspection of composite materials with regard to aeronautical structures is a challenging task. These structures need to be critically examined for the defects, which otherwise would lead to serious consequences. One better way of testing these structures is with Laser Based Ultrasonic (LBU) system. Where ultrasonic waves are generated in parts to be tested to get time of flight information i.e. time of flight information for

different wave modes like pressure, shear and surface waves. After knowing the time of flight, the defects in the examined part can be reconstructed with the tomographic techniques.

1.3 LITERATURE SURVEY

Evaluation of advanced composite materials non-destructively, poses a challenge to researchers and applied technologists. Lasers based Ultrasonic methods, however, are most common and practiced widely because this is the one, that can reach the areas which conventional ultrasonics cannot, and also the amount of information that ultrasonic signals carry. In this work, an overall review of processing of ultrasonic signals to enhance the confidence of identification of shear wave is presented. And also an effort has been made to study the directivity (Radiation) patterns of laser source in aluminum.

Modern non-destructive testing of materials has to provide the mechanism by which the exact location and size of the flaw can be figured out. The simplest acoustical characterization of material deals with the velocity measurements. Scruby and Drain [1] in their introductory book on laser ultrasonics discussed the mechanisms of generating the ultrasonic waves with lasers and detection of them using variety of laser interferometers. Krautkramer and Krautkramer [2] discussed the techniques of measuring the wave speeds of different waves in conventional mode, and hence characterizing the flaws in materials. Arnold et al [3] measured the shear wave velocities in metals. Specially designed Speckle interferometer was used to measure the shear displacements generated by the short laser pulses in aluminum semi cylindrical samples, both in thermo-elastic and ablation regimes and have presented the angular distribution pattern of the amplitudes. The acoustic waves were generated by Q-switched ruby laser. Pengzhi et al [4] studied the directivity patterns of laser thermoelastically generated ultrasound in metal with consideration of thermal conductivity. They obtained the terms contributing to the directivity patterns for longitudinal and shear. And they concluded that, the thermal diffusion does not influence effectively the transverse directivity pattern. Fassbender et al [5] studied, the efficient generation of acoustic pressure waves by short laser pulses in polycrystalline metal samples. The experimental set up consists of Q-switched ruby laser in a multimode configuration to give pulses with gaussian temporal envelope and with a maximum power of 20MW and a maximum energy of 600mJ. The specific power density

I_0 at which only a maximum pressure pulse is generated was calculated. The Fourier spectrum of the pressure pulse was also evaluated. Osama and Wright [6] studied the detection of shear strain pulses with laser Pico-second acoustics. Scruby et al [7] carried out the quantitative studies on thermally generated elastic waves in laser-irradiated metals. A calibrated wide-band detection system, incorporating a capacitance transducer, which could measure acoustic waveforms with minimum distortion, was used. The transfer function of the metal block has been deconvoluted to give the acoustic source function, which was modeled as a rapidly expanding point volume of material. Amplitudes of both shear and pressure waves were found to be proportional to the amount of laser energy absorbed. Dewhurst et al [8] carried out the quantitative investigations to study acoustic generation in metallic samples over a wide range of laser power densities, which includes plasma formation on the target's surface. Additionally, the effect of modifying the metal surface was examined. And concluded that the waveforms obtained in thermo elastic regime are independent of laser energies and power densities. At constant laser energy, the acoustic displacements amplitudes of shear and pressure waves are independent of power density. On increasing the power density to form plasmas, the acoustic displacement waveform changes in shape and amplitude both being dependent on laser power density. Hoffman and Arnold [9] have modeled the ablation source in laser ultrasonics. Aussel and Monchalin [10] have determined the attenuation in ceramic and steel samples making two assumptions. Firstly when the spherical wave approximation holds i.e. for small laser spot sizes, thick samples, or low ultrasonic frequencies. Secondly when the plane wave approximation holds, i.e. large laser spot sizes, thin samples or high ultrasonic frequencies. Jin huang et al [11] characterized the defects in thin plates using laser-based ultrasonics. A laser based ultrasonic system consisted of a tunable narrowband laser line array ultrasound generator and a fiber-optic dual-probe heterodyne interferometer. The defects were constructed with tomographic imaging with lamb waves. Christophe Barriere and Daniel Royer [12] have developed a simple method suitable for extracting the large mechanical displacements from the phase modulation of an optical beam reflected from the moving surface. In the MHz range, transient displacements larger than $1\text{ }\mu\text{m}$ have been measured with a standard heterodyne interferometer. Arnold et al [13] evaluated the condition for efficient generation of surface acoustic waves by thermoelasticity. Wu Yaping et al [14]

studied the directivity of laser-generated ultrasound in solids. By solving the thermoelastic wave equations, they obtained analytic expressions of three-dimensional ultrasound displacements in the far field. And concluded that thermal diffusion, optical absorption, ultrasonic frequency, and the diameter of source all have effects on the directivity. Early attempts by Lord [15] used a green function formalism to obtain the directivity due to thermoelastic source. Rose [16] considered the point source as a surface center of expansion and obtained a formal solution, again using a green function formalism. The theoretical modeling of the thermoelastic source they used took no account of thermal diffusion in to the solid. Cooper [17] and Scruby et al [18] using method similar to that described by Lord and Rose, calculated the expected directivity of the compression and shear wave generated in the thermoelastic regime. Doyle [19] and McDonald [20] considered the thermal diffusion and verified its effects on the ultrasound. More recently, Wu [21] considered both thermal diffusion and optical absorption in the three-dimensional case, and obtained a numerical solution of the epicentral displacement by employing the method of eigen function expansion. Their results showed that both thermal diffusion and optical absorption have effects on the laser-generated ultrasound. Zeljko Andreic[22] studied the shape of the plasma cloud generated by pulsed laser ablation of solid targets when the laser beam impacts onto the target surface at large angles. Time-integrated photographs of the expanding plasma clouds clearly showed that plasma is produced at large impact angles too, and that it always expands perpendicularly to the target surface. Aussel and Monchalín[23] presented a laser-ultrasonic method to measure the acoustic velocities and the elastic constants of solid materials based on the cross correlation of successive echoes. Diffraction corrections are calculated, and dispersion effects are evaluated by frequency analysis. Moushumi Zaman et al [24] analyzed the advanced concepts in time frequency signal processing. They studied the spectrogram explicitly. Ljubisa Stankovic et al [25] proposed a new signal-adaptive joint time-frequency distribution for the analysis of nonstationary signals. It was based on a fractional-Fourier-domain realization of the weighted Wigner-Ville distribution. Improvement over the standard time-frequency representations is achieved when the principal axes of a signal (defined as mutually orthogonal directions in the time-frequency plane for which the width of the signal's fractional power spectrum is minimum or maximum) do not correspond to the time and

frequency. Zbigniew Leonowicz et al [26] proposed a new method of observation and diagnosis of inverter-fed induction motor drives. The spectrum of the space-phasor was estimated with the help of the Wigner-Ville distribution (WVD) and its time-frequency representation with excellent time and frequency resolution. Datta [27] proposed a methodology to experimentally detect defects using a two-dimensional automated Ultrasonic C-scan system. Both time and frequency domain features were extracted from the digitized data during scanning procedure. Multi- dimensional cluster analysis was used for effective grouping of datasets in a systematic manner leading to automatic image generation. Detection of ultrasound by optical means were motivated by the need to visualize and image the ultrasonic field. Sarin [28] and Daliraju [29] have developed an experimental set-up using an Nd: YAG pulsed laser for generation of ultrasound in specimens and a He-Ne continuous laser based heterodyne optical interferometric probe for detection of the same. They have proposed a methodology for inspection of composite specimens using LBU and evaluation of effectiveness of different features of ultrasonic signals in detecting different types of defect. Ramakrishna [30] constructed the defects in composite materials using tomography by measuring the pressure wave time of flight data. The Algebraic Reconstructional Technique was used for reconstructing the defects. Error analysis has been carried out to check the influence of various parameters on reconstructed image. Monchalin et al [31] have demonstrated the applicability of laser ultrasonics to the steel industry: on line thickness gauging of seamless tubes and to the aeronautic industry, inspection of the composite structure of aircrafts.

1.4 PRESENT WORK

The generation of ultrasound by short laser pulses is the base of new technique in non-destructive testing with high potential. Characterization of laser source is necessary to understand the wave propagation phenomenon in either metals or non-metals. . In this work, Q-switched Nd-YAG pulsed laser has been used for the generation of ultrasound in specimens and He-Ne continuous laser based heterodyne interferometer is used for detecting the ultrasonic field. If directivity pattern and attenuation characteristics are known, much progress could be made in identifying the arrival times of either pressure or shear wave, which helps in reconstructing the defects with tomography. So far this was carried out using the time-of- flight data of pressure wave. Because measuring the shear

wave time-of-flight is not as simple as pressure wave with laser interferometry. In order to understand shear waves, as a preliminary step an attempt has been made on Aluminum. In the present work, extensive time-frequency analysis of experimentally obtained signals in aluminum in ablation regime is carried out to characterize pressure and shear waves in ablation regime. After characterizing, the time of flight and the directivity pattern of each wave is evaluated. Experiments were conducted on different radii aluminum semi-cylindrical samples and on a rectangular sample.

1.5 THESIS ORGANISATION

The various chapters in the thesis deal with the following aspects.

Chapter 2 deals with different aspects of laser-based ultrasonic technique and discusses different types of mechanical waves.

Chapter 3 describes the details of the experimental set-up and data acquisition procedure.

Chapter 4 discusses the radiation pattern of laser source and signal processing.

Results and discussion are presented in Chapter 5.

Chapter 6 gives conclusions and scope for future work

Chapter 2

BASICS OF LASER ULTRASONICS

2.1 INTRODUCTION

Laser (Light Amplification by Stimulated Emission of Radiation) is a device that generates or amplifies light, just as transistors generate and amplify electronic signals at audio, radio or microwave frequencies. Here, light must be understood broadly, since lasers have covered radiation at wavelengths ranging from infrared range to ultraviolet and even soft x-ray range. The term ultrasonics is often used to describe mechanical wave propagating in gases, liquids or solids at frequencies above the upper limit of human hearing. Because the characteristics of these waves are influenced by the mechanical properties of any medium through which they pass, hence give scope for exploring the material properties by knowing the changes in the laser properties.

The laser-based ultrasonics (LBU) is the technique, in which laser beam interaction with the surface of the test sample is substituted for piezoelectric transducers for launching and probing elastic waves. Since they do not require any mechanical contact, these techniques are very attractive. For example, in the field of NDT, the association of laser generation with optical detection provides a completely remote ultrasonic system. Other fields of applications are: material evaluation, acoustic emission photo thermal microscopy and acoustic field imaging. Based on the intensity of the laser, the impact generation methods may be classified in to three main categories: thermoelastic regime, constrained surface and ablation régime. In the field of NDT, there are different methods applied; for example, one uses shock waves, which are generated by laser impact on the sample and optical detection (interferometrics or non-interferometrics), which monitors the induced surface. Other methods are used incorporating contact ultrasonic probes working as receivers or transmitters. Hence, this method needs no contact medium and the source can be some meters away; it is used especially for applications such as NDT of systems at high temperature and hostile environments.

2.2 PROPERTIES OF LASER LIGHT

Lasers are characterized by a number of key optical properties, most of which play an important role in the interaction with ultrasonic fields. Their four major optical properties are:

- (1) Monochromaticity
- (2) Coherence
- (3) Directionality
- (4) High Intensity or Brightness

which are inter-related.

2.2.1 Monochromaticity

Monochromatic means the same frequency. Light from sources other than lasers covers a range of frequencies. True single-frequency operation of a gas laser can be achieved by careful design. Multimode operation of course reduces the monochromaticity a laser. A small helium-neon laser generally has three or four longitudinal modes excited with a spacing of a few hundred MHz, depending on the cavity length. This still gives a bandwidth of a few parts in 10^6 . Solid-state lasers tend to have rather large frequency spreads.

Monochromaticity is important for some ultrasonic applications, in particular the interferometric measurement of ultrasonic fields. Firstly, it is necessary in order to obtain high coherence, and secondly, it enables accurate measurements of ultrasonic displacements, since calibration is against the wavelength of the light. Monochromaticity is of less importance for the generation of ultrasound by laser.

2.2.2 Coherence

Coherence means the same order or as a copy of the other photon and in phase with the other photon. Coherence is an important property when it comes to building an optical system to detect ultrasonic waves. In simple words, coherence is used to describe how well a wave disturbance at one point in space or time correlates with the disturbance at another point. If there is a well defined phase relationship between the light at two different points in space (i.e. two light beams), or at two different times (i.e. one beam

split into two with a delay between the parts, as is typical in an interferometer) then the two light disturbances can be brought together to produce a predictable interference pattern. If the light is completely incoherent so that there is no predictable relationship (i.e. random phase) between the two disturbances, no interference fringes will be formed. Fig.2.1 shows the comparison between the ordinary light and laser light.

Coherence is important to the reception of ultrasonic waves by laser. Most techniques involve some form of interferometer, in which good coherence between probe and reference beam is essential. Coherence length is the distance of the origin of the beam to the farthest point at which the wave disturbance can be effectively correlated with the disturbance at its starting point. Conventional monochromatic light cannot be used because their coherence length is only of the order of millimeters. The use of a gas laser however enables use of a longer probe than reference beam. This means that a compact instrument (incorporating all except the probe beam) can be built, and that the distance to the sample is not critical.

2.2.3 Directionality

Directionality is a function of the spatial coherence of the beam of light. Laser beam is highly directional which implies laser light is of very small divergence because of the parallelism of the beam. The radiation produced by a laser is confined to a narrow cone of angles. The beam of divergence for a typical gas laser is of the order of 1 milli-radian, although some commercial He-Ne lasers are available with divergences of a few tenths of a milli-radian. Comparable beam divergences are now available from pulsed solid-state laser systems. It is only possible to attain such low beam divergence from conventional light sources by severe collimation, which leads to extremely low intensities. The diameter of the beam is typically about 1mm for a gas laser such as helium-neon, and in the range 1-20 mm for a pulsed solid-state laser.

The light from gas and solid state lasers thus forms a highly collimated beam which is extremely valuable for laser ultrasonics, since it enables the beam to be focused to a very small spot. This means not only high spatial resolution, but also, in the case of ultrasonic displacement measurement by interferometer, the ability to collect a larger fraction of the scattered light from a rough surface, thereby increasing sensitivity. For laser generation, it indicates that very high incident power densities are attainable. Low

beam divergence also means that the beam can travel distances of the order of several meters from the laser to the specimen without appreciable spreading and losses. Thus both laser generation and reception of ultrasound can be made a genuine remote techniques.

2.2.4 High Intensity or Brightness

Intensity or brightness of a light source is defined as the power emitted per unit area per unit solid angle. A laser beam is extremely intense, more intense than any other light source. This is perhaps the property for which lasers are best known outside the field of optics. Although the optical power output from a small helium-neon (He-Ne) laser may only be say 2mW, a beam diameter of 0.5mm leads to a power density of about 1 W cm^{-2} . Such a beam can readily be focused by a simple lens to a spot of diameter 0.05 mm because it is monochromatic and coherent. Focusing optics produces a beam of sufficient intensity to melt, cut or weld structural materials.

Intensity is a most important property for laser reception of ultrasound, as sensitivity of a single mode laser interferometer system (defined as signal to noise ratio for a fixed bandwidth) increases with the square root of light intensity, provided other conditions remain constant. The limiting factor becomes the intensity at which the specimen is damaged or otherwise adversely affected by intense irradiation. Increase in power also brings penalties like increase in noise and multimode interference. Intensity is also a crucial factor in the generation of ultrasound by laser since incident power intensities typically in the range of 10^4 - 10^6 Wcm^{-2} are needed to act as a thermoelastic source of ultrasound. Above 10^7 Wcm^{-2} , it is ablation regime. The laser energy per pulse largely controls the ultrasonic amplitude in the thermoelastic and ablation regime. The limiting factor is not the power that is available from commercial lasers, but rather the threshold for damage in the irradiated sample. Indeed, many pulsed lasers are too powerful for ultrasonic applications, and must be used at reduced power if the technique is not to be destructive.

2.3 BASIC PRINCIPLE OF LASER OPERATION

The laser is a device, which amplifies the intensity of light by means of a quantum process known as stimulated emission. A practical laser needs a means of amplification (i.e. stimulated emission) and a means for feeding the energy back into the system to build up sustained oscillation. The operation of the simplest type of laser can be most readily understood in terms of a quantum mechanical model having say three energy levels E_0 , E_1 , E_2 , such that $E_2 > E_1 > E_0$ (Fig.2.2). In reality, there may be more than three levels, but for present purposes, other levels are neglected. The ground state E_0 is well populated, whereas the intermediate and upper states are more sparsely populated. Suppose now the atom absorbs a quantum of incident radiation such that the atom is excited into the upper state. From quantum theory, the radiation must have a frequency ν_p such that

$$h\nu_p = E_2 - E_0 \quad (2.1)$$

Where h is the Planck's constant. In laser terminology this process of absorption is known as 'pumping', so that ν_p is the 'pumping frequency'. Pumping tends to equalize the population of two states so that E_2 becomes well populated. This reverses the normal occupancy of E_2 and E_1 and is known as population inversion. Emission (i.e. stimulated emission) can now occur in response to incident radiation, at a frequency ν given by

$$h\nu = E_2 - E_1 \quad (2.2)$$

It can be noted that necessarily $\nu_p \geq \nu$, so that the pumping frequency must always be equal to or higher than that of the radiation to be amplified. In order to obtain light of sufficient intensity for practical use, there has to be some mechanism for feeding the energy back into the laser system and thereby building up the amplitude of oscillations in a resonant system. The usual way of obtaining sustained oscillations is to site a high performance mirror at each end of the lasing medium. In the simplest system, both mirrors are plane, and accurately aligned perpendicular to the axis of the laser. Thus, the light can be reflected backwards and forwards through the lasing medium. On each pass it stimulates further emission from the medium and is thus amplified in intensity.

2.4 LASERS FOR ULTRASOUND GENERATION

The simple laser arrangement will operate in a pulsed mode if it is pumped for example by a pulsed flash tube. Depending on the type of laser, pulses of duration typically 100 μ s to 1ms can be obtained. Although high-energy pulses can be produced in this way, the normal mode is not particularly useful for laser ultrasonics, because the pulse duration is too large. An additional technique, known as Q-switching or Q-spilling, is needed to obtain pulses in the required 1-100ns range. The Q (quality) factor of a cavity resonator is the energy stored in the cavity divided by the energy lost from the cavity per round trip of the light within the cavity. Thus, if Q is low, the cavity oscillations are suppressed and the stored energy builds up within the lasing medium. When the Q is high, the cavity can support oscillations into which energy is supplied from the medium. Thus switching from low to high Q results in the rapid extraction of power from the laser cavity. Practical Q-switches are in the form of elements with variable absorption that are inserted between the mirrors. Two commonly used Q switches are the Pockels cell and bleachable (saturable) dye. Also of potential importance to non-contact ultrasonics are lasers that can be pulsed repeatedly. Adequate cooling in pulsed solid-state lasers is a problem. Hence gas lasers are preferred. However solid-state lasers can store higher individual pulse energies than gas medium lasers. Conventional ultrasonic inspection often uses repetition rates as high as 1-10 kHz for signal averaging purposes or for speed.

Laser generation of ultrasound does not impose very stringent conditions on the source laser. All that is required is the ability to deliver a reasonably high-pulsed energy density to a small area of the specimen, where the pulse length is in the range of 1-100 ns. As already mentioned, wavelength is not critical, nor is monochromaticity or coherence. Most researchers have employed a solid state laser, either ruby or Nd: YAG. The Nd: YAG laser has proved itself to be a versatile system under Q-switched conditions. Adequate pulse energy can be obtained from Nd: YAG lasers of modest size, while the pulse lengths are close to ideal for ultrasonic studies in metals. However, the fundamental wavelength (1064nm) is in the near infrared, which makes alignment more difficult than with a visible laser, in addition to increasing the risk of accidental eye damage. The Nd: YAG laser is available with frequency doubling to give several harmonics of the

fundamental frequency. The frequency-doubled wavelength of 532 nm is in the middle of the visible spectrum, while the harmonics of 266nm and 355nm are in the ultraviolet zone.

2.5 LASERS FOR INTERFEROMETRY

For applications like interferometry, where wavelength purity and coherence are important, continuous wave lasers are to be designed with special optical components. The main problem is that a simple laser will excite a number of longitudinal and transverse modes. The result is that energy is amplified over a narrow range of frequencies instead of the desired single frequency, giving rise to inter-mode beat frequencies, and there is a variable distribution of energy across the beam. The generally preferred transverse mode (usually the lowest order mode with circular symmetry, TEM₀₀) can be selected, and higher order modes are suppressed, by the use of at least one curved (concave) mirror at the end of the cavity and/or a suitable aperture within the cavity. A multi-mode laser can be employed to minimize the multi-mode problem of longitudinal wavelengths in interferometry and then a balanced detection system and adjustment of the path difference between the two arms of the interferometer can be used to minimize the effects of inter-mode beats if necessary.

The reception of ultrasound by laser is dependent upon all the fundamental properties of the laser: monochromaticity, coherence, directionality and high power density. Because of its ready availability and excellent optical characteristics, notably monochromaticity and coherence, the He-Ne laser has dominated much of the work. This system is however somewhat limited with regard to maximum power which controls sensitivity. The other choice is the argon ion laser, which not only can deliver higher power, but also inherently more sensitive because of its shorter wavelength. Argon ion lasers are however very bulky and noisy. The CW Nd: YAG laser is also available which falls in to solid-state option, although it suffers from a number of drawbacks including bulk.

2.6 LASER-IRRADIATED ULTRASOUND MODES

Laser ultrasonics is based on the phenomenon that laser irradiation onto a solid surface generates ultrasound waves in the solid. Fully non-contact generation and detection of ultrasonic waves can be realized by combining with optical (laser) interferometer for ultrasonic detection. Thus, laser ultrasonic NDE could be applied to materials and structures in hostile environments, such as very high temperatures, or to components having complex geometries. A laser emits a beam of coherent radiation, whose wavelength may be in the infrared, visible or ultraviolet part of the electromagnetic spectrum. When this is incident on a solid sample, in general some of the energy is absorbed by various mechanisms, depending upon the nature of the sample and the frequency of the radiation, while the remainder is reflected or scattered from the surface. Three basic mechanisms have been described below:

2.6.1 The Thermoelastic Regime: At low power densities, the absorption of the light by the material causes the temperature to rise locally near the surface of the inspected component. By thermal expansion, the heat generated by optical absorption creates a stress distribution near the surface of the material, at the point of impact of the incident light as in Fig 2.3. The stress distribution, which can be represented by an ensemble of buried thermoelastic sources, is itself at the origin of a high frequency ultrasonic pulse propagating inside the material. As the heat injected into the material dissipates, the component's surface returns to its original state, undamaged by the generation process. Laser generation of ultrasound in the thermoelastic regime is a nondestructive process. For typical Q-switched laser pulse durations, the thermal wave field only extends a few micrometers even in good conductors. Contrast the incidence of low frequency modulated light where the thermal field extends millimeters or centimeters and is itself useful for materials characterization.

2.6.2 The Constrained Surface Source: Constrained surfaces include coating the surface with a thin solid layer of, for instance, paint or rust and roughness, covering the surface with a transparent solid such as glass, covering the surface with a transparent liquid, and finally constraining a thin layer of liquid between a transparent solid and the

sample. All these four techniques for modifying the surface of the sample introduce large stresses normal to the surface, as shown in Figs.2.4 (a-d), which are otherwise absent for the thermo elastic source at a free source. The form of the ultrasonic source is thus substantially modified. The different combination of stresses generates a different ultrasonic sound field, with considerable enhancement in compression-wave amplitude, especially propagating normal to the surface. The constrained surface source generates a sound field more akin to that of ablation, but at lower power densities and without any damage. However, the need to constrain with for instance a liquid, reduce the usefulness of the laser ultrasonic source for many non-destructive applications.

2.6.3 The Plasma (ablation) Regime: At higher incident powers, surface melting and evaporation occurs, resulting in material ablation and the formation of plasma above the sample surface as shown in Fig.2.5. The momentum of the evaporated material exerts an opposite force on the sample, causing a reactive stress at the surface. This generates an intense broadband ultrasonic source, whose strongest components are, directed normal to the surface. The effects caused by the plasma generated in association with ablation in case of Q-switched lasers are:

- The plasma exerts a high pressure on the surface, which in turn suppresses vaporization of the material by raising the boiling point of the material well above its normal value.
- It absorbs light from the laser pulse, acting as a shield, but also becoming extremely hot.
- As it expands it produces an impulse reaction on the surface.
- It radiates some of its heat back on to the surface, maintaining its high temperature for some time after the incident laser pulse power has started to fall.

2.7 PRINCIPLE OF LASER INTERFEROMETRY

Optical interferometry is a very sensitive way of measuring displacement, but to be practicable for general use, it requires a highly monochromatic light source and thus the use of lasers is virtually essential. Interferometers for the detection of ultrasonic movements of waves may be divided into two main types. In the first type, light scattered

or reflected from a surface is made to interfere with a reference beam, thus giving a measure of optical phase and hence instantaneous surface displacement. The second type of interferometer makes use of interference between a large number of reflected beams. This is designed as a high-resolution optical spectrometer to detect changes in the frequency of the scattered or reflected light. It thus gives an output dependent on the velocity of the surface. The first type is the more widely used and the most practical at lower frequencies and with reflecting surfaces. The second type offers a potentially higher sensitivity with rough surfaces, particularly at higher frequencies.

For the detection of ultrasonic waves at a surface, the techniques are admittedly insensitive compared with piezoelectric devices. They do, however, offer a number of advantages.

- (1) They are non-contacting and thus do not disturb the ultrasonic field. The point of measurement may be quickly moved and there are no fundamental restrictions on surface temperature.
- (2) High spatial resolution may be obtained without reducing sensitivity. The measurements may be localized over a few micrometers if necessary.
- (3) As the measurements may be directly related to the wavelength of the light, no other calibration is required.
- (4) They can have a flat broadband frequency response, something difficult to achieve with piezoelectric transducers, particularly at high frequencies.

2.8 HE-NE LASER HETERODYNE INTERFEROMETER

2.8.1 Working of Optical Heterodyne Probe

The system consists of a compact optical head and an electronic signal-processing unit. The optical layout is shown in Fig. 2.6. The laser beam emitted by the laser source, horizontally polarized, is directed in the interferometer by two deflecting mirrors. The laser beam is split into two parts by the beam-splitting cube. The *reference* beam is reflected by the beam-splitting cube and goes through the Dove prism. It is then transmitted by the polarizing beam-splitting cube and deflected by the mirror on the photo-detector. The *probe* beam is transmitted by the beam-splitting cube and is

horizontally polarized. Its optical frequency is shifted in the Bragg cell, and transmitted by the polarizing beam-splitting cube. A quarter wave plate transforms the horizontal polarization into circular polarization. The lens focuses the beam on the surface of the sample.

The probe beam is then phase modulated upon reflection on the sample by the mechanical displacement. After the second pass in the quarter wave plate, the direction of polarization becomes vertical. The probe beam is reflected by the polarizing beam-splitter on the photo-detector. Just after the polarizing beam-splitter, the polarization of the probe and reference beam are respectively vertical and horizontal. These two beams can therefore not interfere. The analyzer selects a common component at 45° of the two polarizations, thus allowing interference. The photo-detector delivers a beat signal at the frequency of the Bragg cell phase modulated by the mechanical displacement of the object.

2.8.2 Principle of Detection

The complex amplitude of a laser beam of frequency f_L can be written as:

$$L = e^{2i\pi f_L t} \quad (2.3)$$

This is divided in the interferometer into a reference beam and a signal beam, whose complex amplitude is:

$$R = r.e^{2i\pi f_L t} \quad (2.4)$$

The reference beam does not experience any perturbation, however the signal beam experiences a frequency shift f_B in the Bragg cell. Upon reflection on the object, its phase is modulated by the displacement of the sample:

$$\varphi(t) = 4\pi.d(t)/\lambda \quad (2.5)$$

where, λ is the wavelength of the laser beam and $d(t)$ the mechanical displacement of the object. The complex amplitude of the signal beam is therefore:

$$S = s.e^{2i\pi f_L t + 2i\pi f_B t + i\varphi(t)} \quad (2.6)$$

The interference of the two beams on the photo-detector produces an electrical signal at frequency f_B , phase modulated by the displacement of the object:

$$I(t) = I_0 + i(t) \quad (2.7)$$

$$I(t) = k \cos(2\pi f_B t + \phi(t)) \quad (2.8)$$

The useful signal is contained in the signal delivered by the photo-detector as a phase modulation of the carrier frequency. The signal processor delivers an electric signal proportional to the displacement of the object. Half of the current $i(t)$ is filtered at the frequency f_B , and phase shifted by 90° . It is then mixed with the other half, non perturbed, and yields a current:

$$j(t) \propto \cos(2\pi f_B t + \phi(t)) \times \cos(2\pi f_B t + \pi/2) \quad (2.9)$$

$$j(t) \propto 1/2 [\cos(4\pi f_B t + \phi(t) + \pi/2) + \cos(\phi(t) + \pi/2)] \quad (2.10)$$

The signal at the frequency $2f_B$ is filtered, to give:

$$s(t) \propto \sin \phi(t) \quad (2.11)$$

If the displacement is very small compared to the optical wavelength, this signal can be written as:

$$s(t) = k \cdot 4\pi \cdot d(t) / \lambda \quad (2.12)$$

The final electrical signal is therefore directly proportional to the displacement of the object.

2.8.3 Sensitivity

Laser ultrasonics suffers from a lack of sensitivity relative to conventional ultrasonics as the photon structure imposes a fundamental limit on the change in light levels during generation / detection of lasers.

Overall sensitivity to flaws is given by:

$$\text{Sensitivity} = T \times f(\sigma, A) \times R \quad (2.13)$$

Where T , $f(\sigma, A)$, R are terms related to the transmitted sound, the focal or imaging properties of the system determined by the flaw scattering σ and the focal aperture A , and the receiver sensitivity. The generated signal can be improved using tailored surface coatings or by increasing the power of the generating source. However, this approach is limited by the onset of ablation in the target.

2.9 TYPES OF ULTRASONIC WAVES

Ultrasonic waves are waves, which occur in matter. A wave is a disturbance of a medium, which transports energy through the medium without permanently transporting matter. In

a wave, particles of the medium are temporarily displaced and then return to their original position. There are a variety of ways to categorize waves. One way to categorize waves is to say that there are longitudinal and transverse waves.

2.9.1 longitudinal waves: longitudinal waves are waves that transport energy in the same direction as the disturbance in the medium of propagation. In a longitudinal wave, particles of the medium are displaced in a direction parallel to energy transport. These waves can be generated in solids, liquids and gases. In isotropic materials the velocity of the longitudinal wave is given in terms of lames constants as

$$v_l = \sqrt{\frac{\lambda + 2\mu}{\rho}} \quad (2.14)$$

2.9.2 Transverse waves: For transverse waves the displacement of the medium is perpendicular to the direction of propagation of the wave. Transverse waves cannot propagate in a gas or a liquid because there is no mechanism for driving motion perpendicular to the propagation of the wave. These waves are also called as shear waves. In isotropic materials its velocity in terms of lames constants is given by

$$v_t = \sqrt{\frac{\mu}{\rho}} \quad (2.15)$$

2.10 CLOSURE

In this Chapter, the basic theory of generation of ultrasonic waves by lasers and their detection using laser-based interferometers has been presented.. Some of the important properties of lasers related to aspects of generation and detection of ultrasonic waves have been discussed. Advantages of using laser-based detectors despite poor detectivity and sensitivity have also been explained. Different types of mechanical waves are explained.

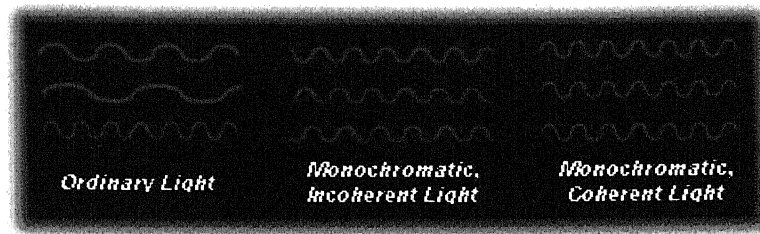


Fig.2.1 Comparison of ordinary light and laser light.

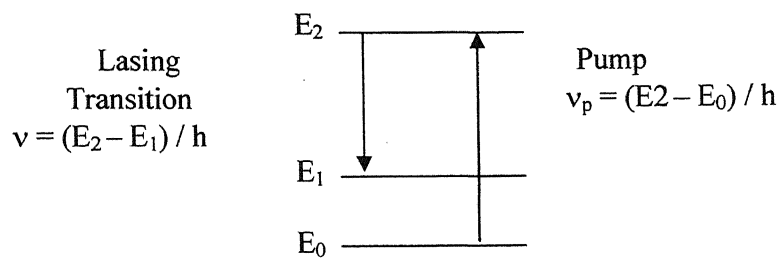


Fig.2.2 Simplified energy level diagram for a laser medium

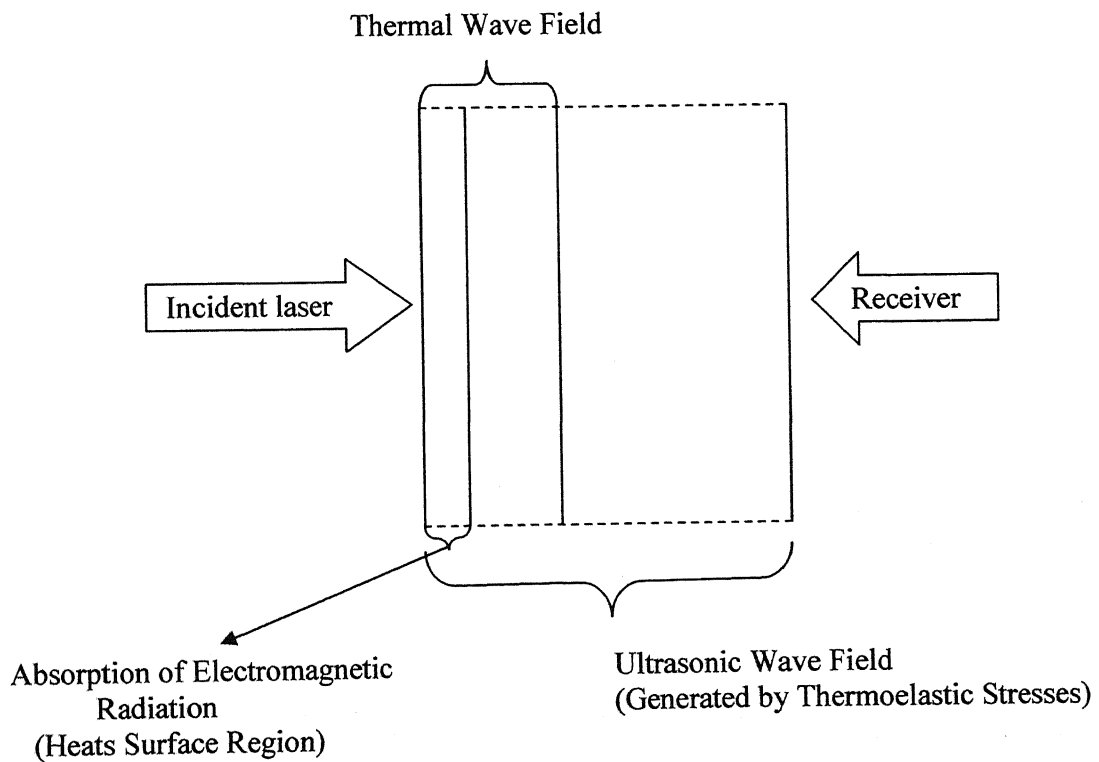
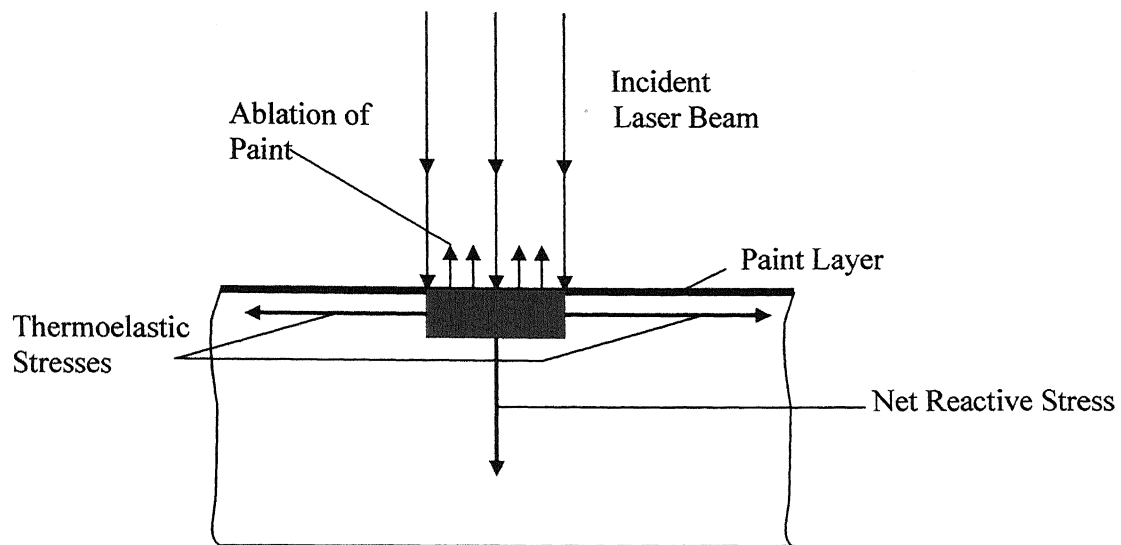
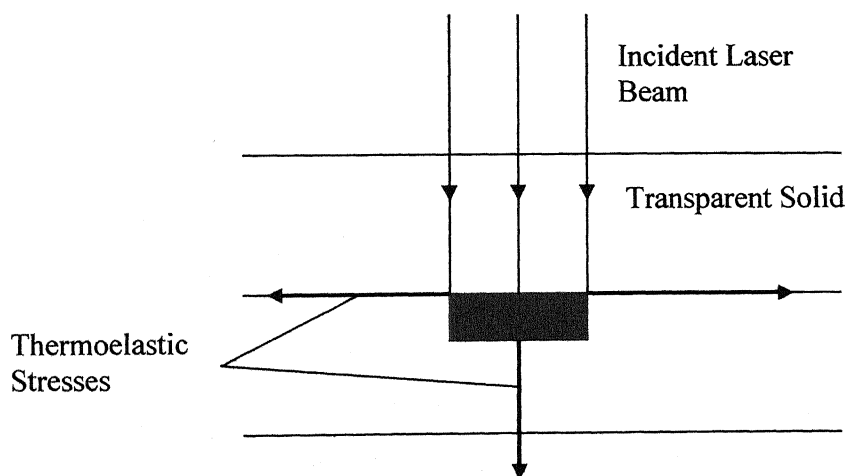


Fig.2.3 Thermoelastic regime



(a) Paint Layer



(b) Solid constraining layer

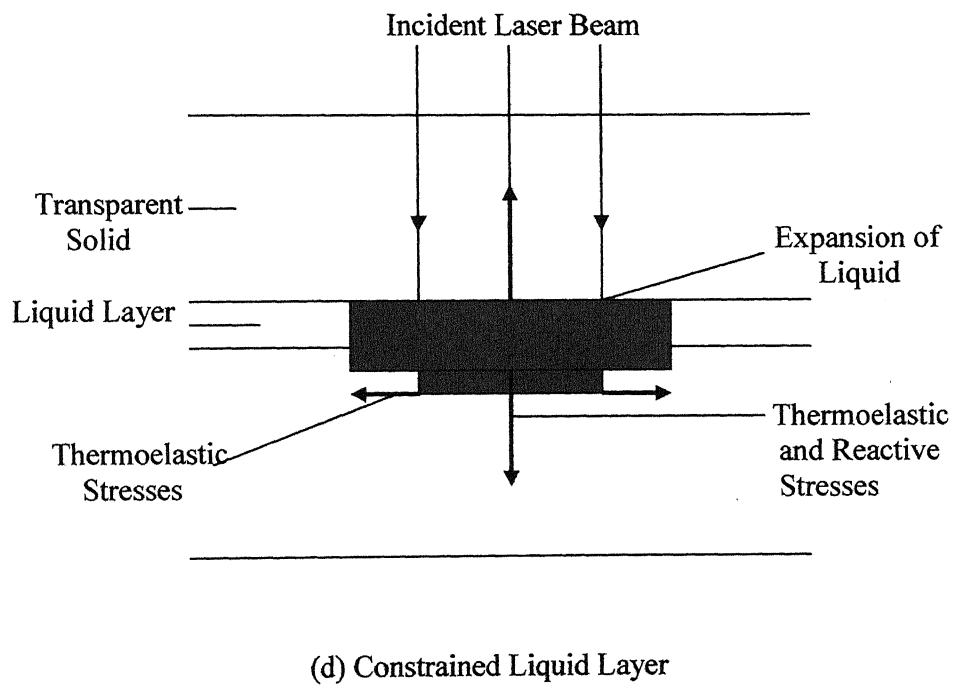
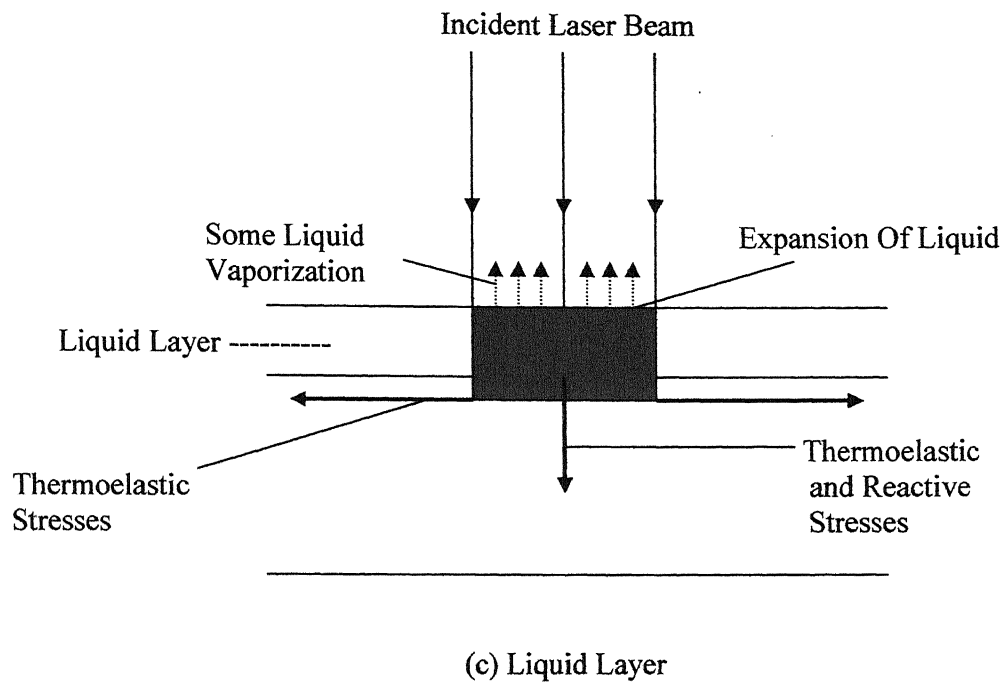


Fig.2.4 Schematic diagram showing stresses induced when a laser pulse is incident on a sample surface covered by (a) a thin layer of paint, (b) a thick transparent solid (c) a layer of liquid (d) a layer of liquid constrained by a transparent solid

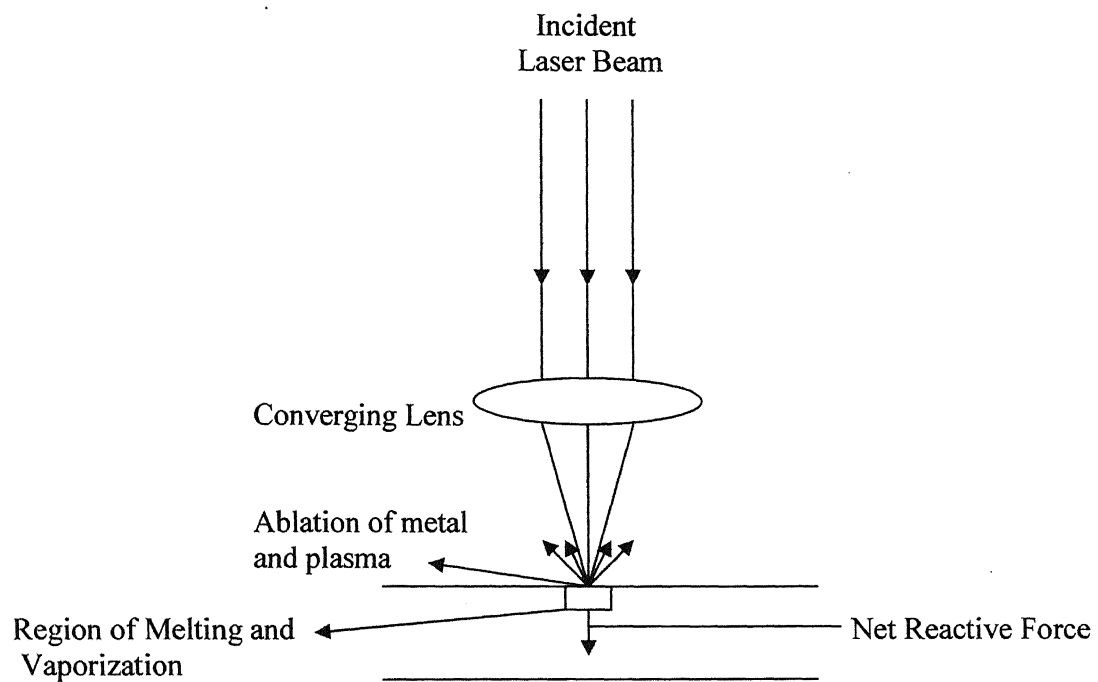


Fig.2.5 Schematic diagram to show ablation of surface material and net reactive force on sample

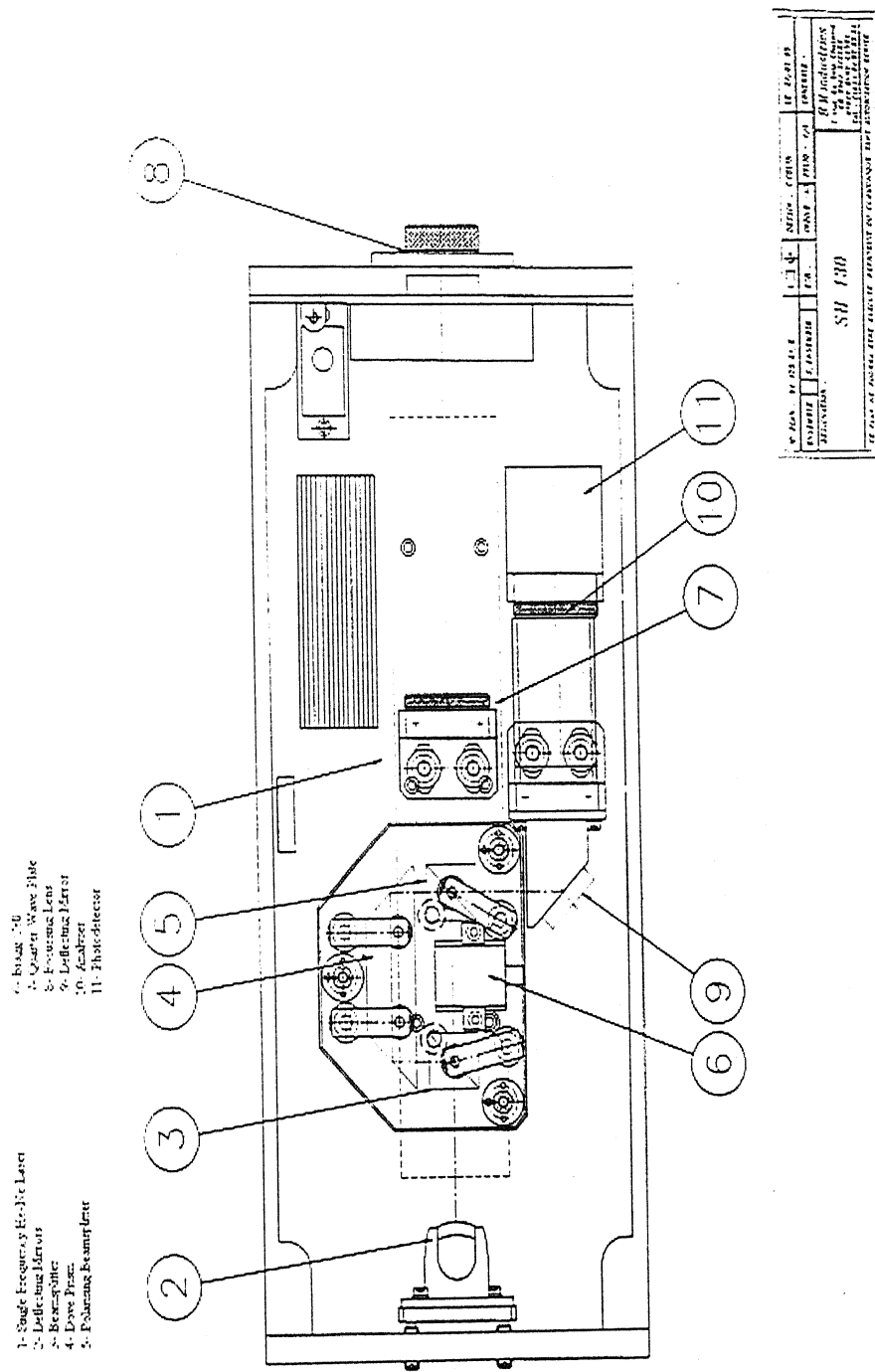


Fig.2.6 Layout of Optical Heterodyne Interferometer

Chapter 3

EXPERIMENTAL SET-UP AND PROCEDURE

This chapter briefly describes the details of laser-based ultrasonic (LBU) set-up, developed for non-destructive evaluation (NDE) of metals and composite materials and data acquisition procedure.

3.1 EXPERIMENTAL SET-UP: LASER-BASED ULTRASONICS

Nd: YAG pulsed laser is used to generate ultrasonic waves in materials or objects to be inspected. Optical Heterodyne type laser interferometer is used to detect the transmitted acoustic field through the material; the signals are then amplified and digitized using a Yokogawa DL1740 Digital Storage Oscilloscope (DSO). The oscilloscope is triggered using a synchronization signal from the pockels cell of the pulsed laser. The recorded waveforms through DSO are transferred over an Ethernet interface for subsequent storage and analysis. The schematic layout of experimental set-up is shown in Fig.3.1 and photographs of the same are shown in Figs.3.2 (a) and (b). The scanning is done manually using two single axis micrometer controlled XYZ translator mounted on the Optical Test Bench. A brief description of the components of the present set-up is given in the following paragraphs.

3.1.1 Nd: YAG Pulsed Laser Ultrasonic Generator

The 5000 DNS series pulsed Nd: YAG laser is built on a modular concept. The optical configuration allows variable setting of the optical parameters. It consists of three major components, the laser-head, the power supply and the cooling unit. The heart of the system is the pumping structure, which houses the Nd: YAG rod and the flash lamp. The lasers are built on an electro-optically Q-switched oscillator. This oscillator uses a pockels cell Q-switch to produce pulses of high intensity and short duration (i.e. in the order of 5-7 ns). Q-Switched lasers are often used as a non-contact ultrasound source in non-destructive testing (NDT) of materials. Q-switched lasers typically have nanosecond (ns) pulse durations and generate broadband ultrasound waves, though longer laser pulses of 100 microseconds or greater have been used for NDE. A variable reflectivity output

coupler allows the extraction of high energy on a single spatial transverse mode. This leads to laser beams of low divergence, and to high conversion efficiencies in the harmonic wavelengths (1064, 532, 355, 266 nm). Different harmonic generators extend the wavelength range to the second, third and fourth harmonics.

The active medium of the laser operates on transitions of triply ionized Neodymium atoms (Nd^{3+}), which take place of another ion (Yttrium) in the host: Yttrium Aluminum Garnet known by the acronym YAG. The laser operates as a 4-level system. The intense broad-spectrum light of the flash lamp populates the upper level. Once in the higher energy level, the Neodymium ions drop to a metastable level, producing a population inversion. The lower level decays by a fast non-radiative process to the ground state. The strongest Neodymium line is 1064 nm.

3.1.2 Optical Heterodyne Laser (He-Ne) Probe.

The SH-130 probe is designed to measure transient mechanical displacements of very low amplitude. It is specially devoted to measure displacements generated by the propagation of an acoustic or ultrasonic wave. The system consists of a compact optical head and an electronic signal-processing unit. The optical head integrates high stability, low power laser source for fast detection with a high spatial resolution.

The electronic signal processor delivers a response proportional to the displacement of the target, with a high bandwidth. The output signal is automatically calibrated to give the absolute value of the measured displacement. The principle of detection (heterodyne interferometry) makes the system insensitive to external vibrations. The compactness of the system allows for a wide range of operating conditions.

3.1.3 Digital Storage Oscilloscope

The set-up utilizes a Yokogawa DL1740 (four channel, one GSa/sec, 500 MHz) Digital Storage Oscilloscope, having built in Zip drive, Ethernet, USB, GPIB and Serial Ports for communication with external PC's/ systems.

3.2 EXPERIMENTAL PROCEDURE (LBU)

3.2.1 Calibration of Set-up.

The system was checked for calibration before scanning the specimen. The procedural steps involved to check for calibration are as follows:

- (1) Alignment of the SH-130 Optical Probe: This involved optimizing the control signal by adjusting the orientation of highly reflective mirror and fine-adjustment of its distance from the focusing lens. (The focal length of the focusing lens is around 215 mm.)
- (2) The photodetector output was measured without going through the signal processor. This was found to be 310 mV (as per specifications). The DSO image is shown in Appendix 'A'.
- (3) The output was then taken through the signal processor with the automatic gain control switched on. The measured signal was found to be in excess of the stipulated signal level of 630 mV peak to peak on 50 Ω (found to be 730 mV). This was adjusted using the adjustments available in the signal-processing unit. The DSO image is shown in Appendix 'B'.

3.2.2 Scanning Procedure

The specimen to be investigated was cleaned and the area under investigation was marked. To get good signals, the portion of the specimen facing to the Ne-He laser was pasted with reflective tape. The He-Ne laser was switched on to align the CW laser beam with the marked point of investigation to obtain good information regarding the wave propagation. Then the Nd: YAG laser was focused onto the specimen using an arrangement of optical mirrors and lenses, so that it acts as a point source and is perpendicular to the irradiated face of the specimen. The alignment of Nd: YAG and He-Ne laser was ensured by focusing the Nd: YAG laser on the marked point of investigation on the opposite face of the specimen. The power level of the laser was adjusted to produce ablation in the aluminum specimen. The scanning was performed at setting corresponding to 1064nm wavelength for the Nd: YAG laser. The He-Ne laser was focused on the opposite side of the specimen at the focal length of the collection lens (approx 215mm). The output of the Optical probe was fed to the electronic signal-

processing unit. The electronic signal processor delivers a response proportional to the displacement of the target, with a high bandwidth. The output signal was automatically calibrated to give the absolute value of the measured displacement. This was fed to the Digital Storage oscilloscope (DSO) where it was displayed and storage of the data was carried out on-line in the PC interfaced to the DSO.

3.3 CLOSURE

In this Chapter, the details of experimental set-up and scanning procedure are presented for the Laser-Based Ultrasonic (LBU) set-up. Experimental procedure for data acquisition is also explained.

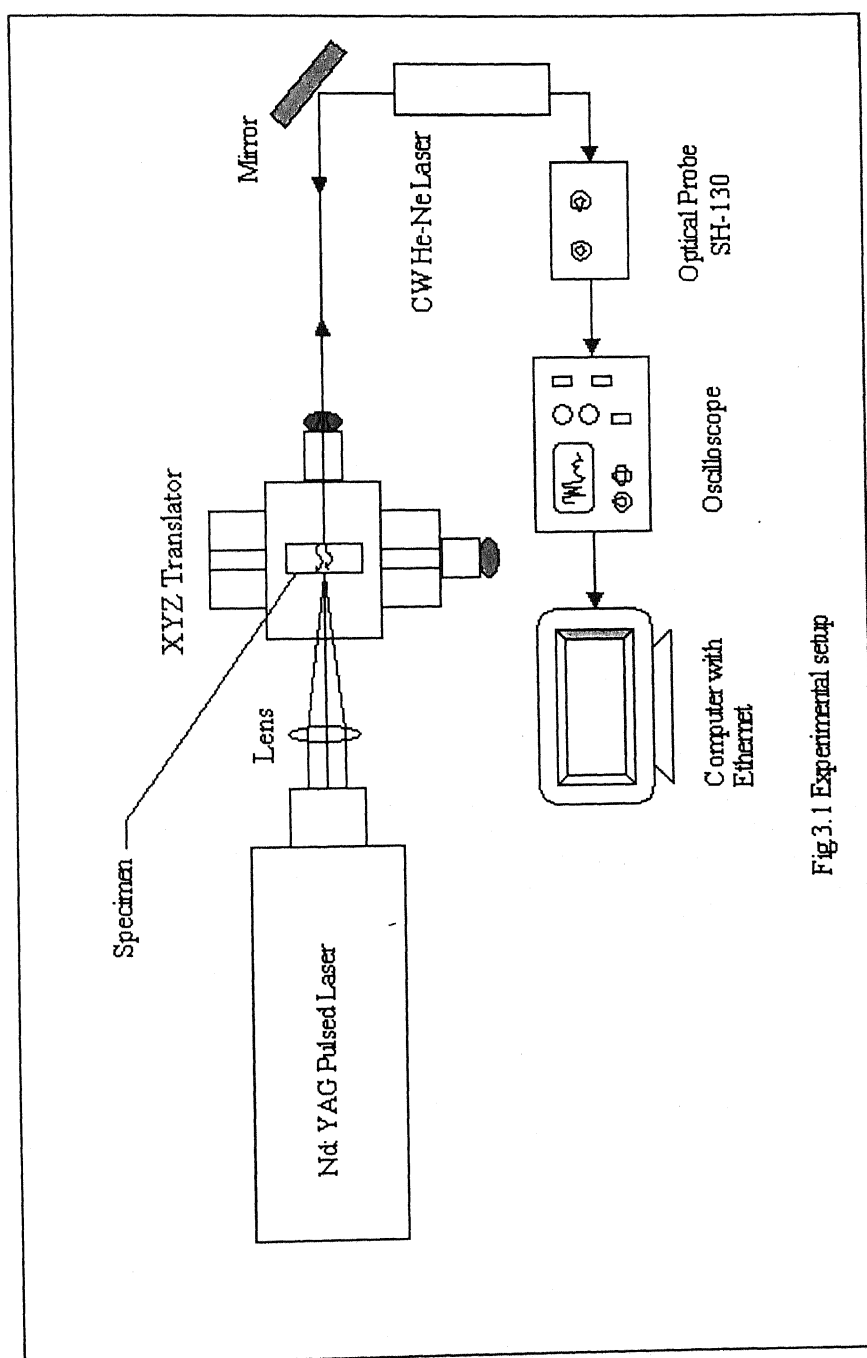


Fig 3.1 Experimental setup

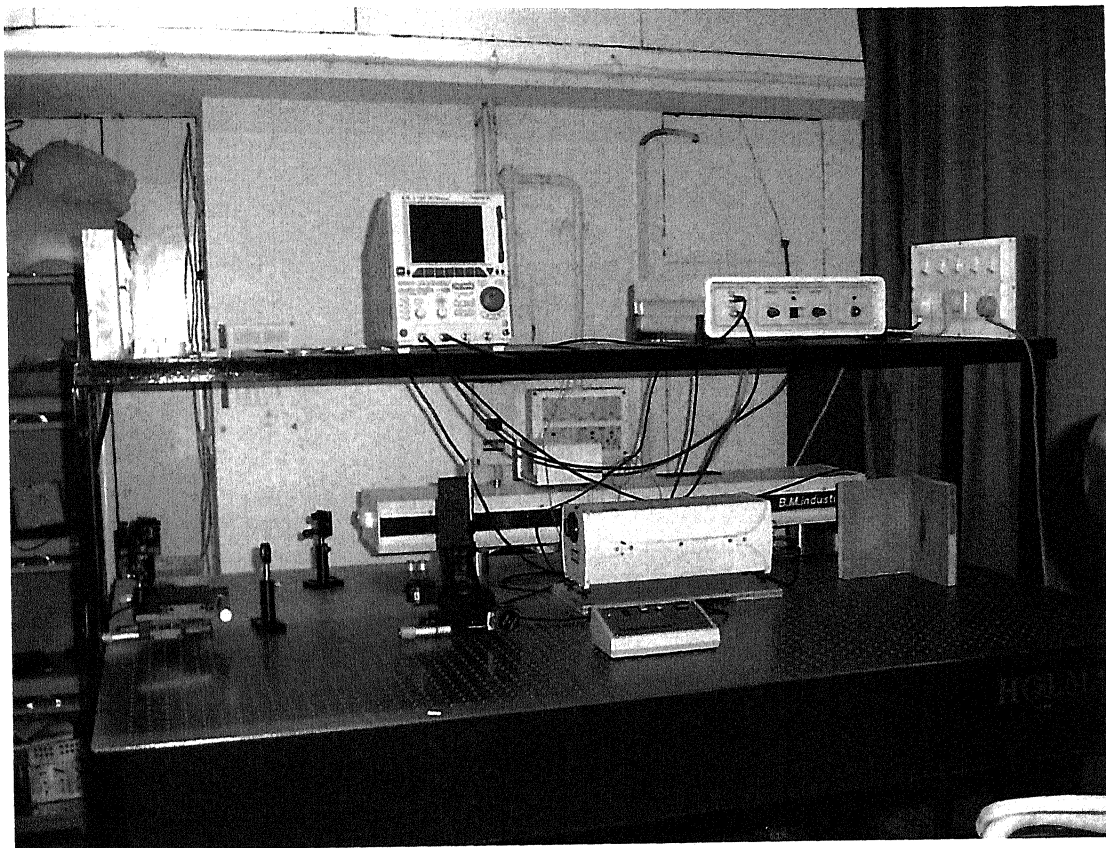


Fig.3.2 (a) Photograph of experimental set-up

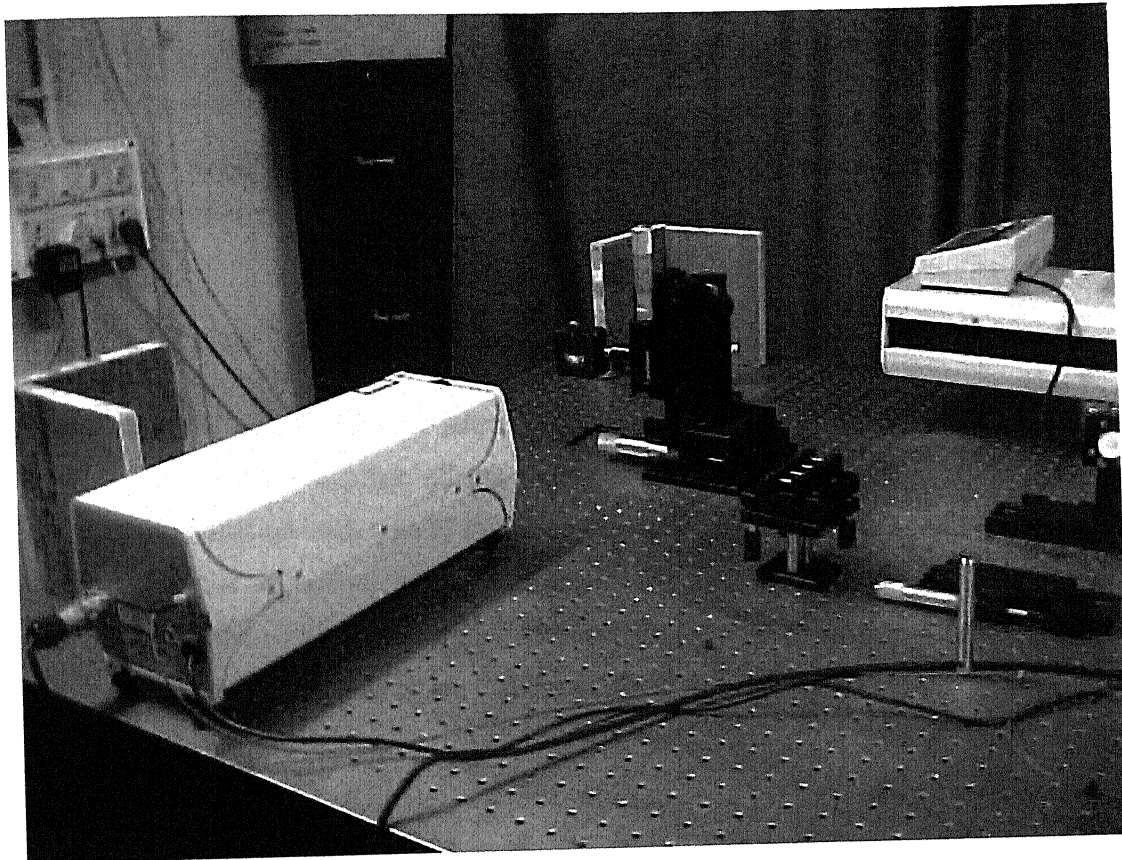


Fig.3.2 (b) Photograph of experimental set-up

Chapter 4

RADIATION PATTERNS AND SIGNAL PROCESSING

This chapter first discusses the radiation patterns of laser sources for pressure and shear wave modes in ablation regime, with a point source assumption. Secondly it looks in to various aspects of signal processing techniques.

4.1 RADIATION PATTERNS FOR LASER ULTRASONIC SOURCES

The laser generation of ultrasound takes place at, or close to, the surface of the solids. Boundary conditions and other effects must therefore be taken into account when calculating the radiation each type of source produces. When a laser beam is employed to produce ultrasound in solids, various characteristic elastic waveforms can be excited, depending upon the optical, thermal, elastic, and geometrical features of the material. Predicting the epicentral displacement and the directivity.

4.1.1 Ablation source

Assuming that when ablation occurs, thermoelastic stresses (which would always accompany ablation in practice) are so small that they can be neglected. Then ablation can be represented as time-varying force acting normal to the surface. The approximation to a point source is likely to be a good one in most situations, since focusing the laser pulse to very small dimensions produces ablation. The angular dependences of the compression and shear waves for the ablation source as given by Hutchins et al [8] are as follows.

for pressure wave,

$$u_r(\theta) = \frac{2k^2 \cos \theta (k^2 - 2 \sin^2 \theta)}{(k^2 - 2 \sin^2 \theta)^2 + 4 \sin^2 \theta (1 - \sin^2 \theta)^{1/2} (k^2 - \sin^2 \theta)^{1/2}} \quad (4.1)$$

for shear wave

$$u_\theta(\theta) = \frac{\sin 2\theta (1 - k^2 \sin^2 \theta)^{1/2}}{k(1 - 2 \sin^2 \theta)^2 + 4 \sin^2 \theta (1 - \sin^2 \theta)^{1/2} (1 - k^2 \sin^2 \theta)^{1/2}} \quad (4.2)$$

where θ is the angle of incident of laser source, and k is the ratio of velocities. i.e. the ratio of pressure wave velocity to shear wave velocity. u_r is the displacement of point of measurement in radial direction and u_θ is the displacement of point of measurement in θ direction. Taking the value of k as 2, for aluminum the directivity pattern of pressure wave and shear wave can be drawn as shown in fig 4.1 and 4.2.

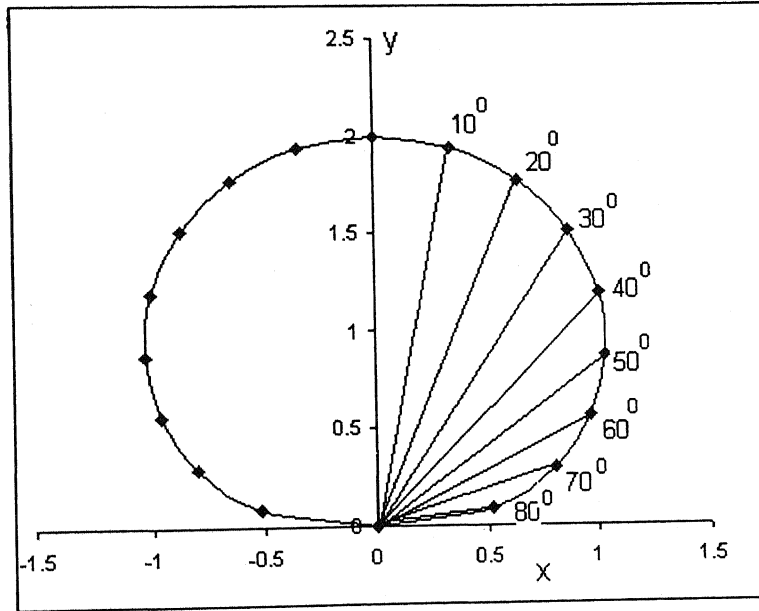


Fig 4.1 Theoretical Directivity of Pressure wave in aluminum

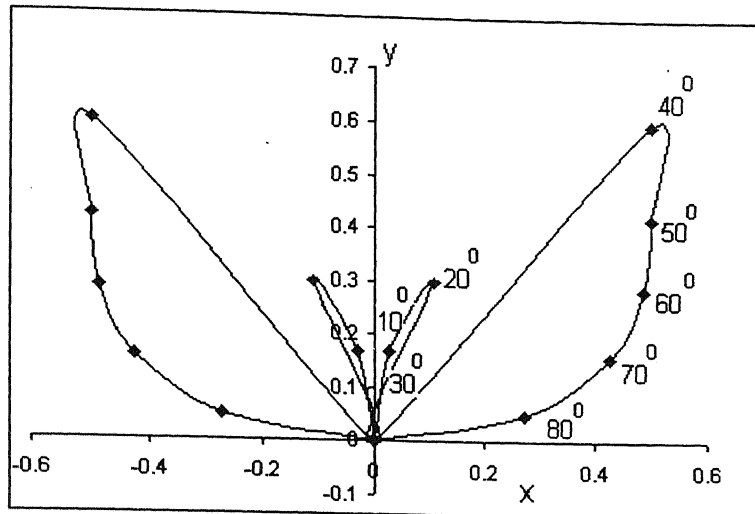


Fig 4.2 Theoretical Directivity pattern of shear wave aluminum

4.2 SIGNAL PROCESSING

The field of time-frequency signal analysis is one of the recent developments, which provides suitable tools for analyzing non-stationary signals. Non-stationary signals are characterized by a time-varying spectral content.

Classical signal processing techniques such as the Fourier transform (FT) are not adequate for analyzing the time-varying signals, which are signals whose frequency content changes with time. These signals are important as they naturally occur in many real world applications. Time-frequency representations (TFRs) are specifically designed to process time-varying signals as they jointly display time and frequency information demonstrating which frequencies occur at a certain time, or at which times a certain frequency occurs. Among many TFRs developed in the literature, the spectrogram is a popular signal-processing tool. Compared to analog signal processing techniques, digital signal processing technique has advantages. To identify a particular damage type, specific information in the form of features, need to be extracted. Each type of damage interacts with the signal in a unique way. These interactions must be found and quantified for defect identification process. By processing the signals digitally, one can obtain information regarding the wave mode. i.e. pressure or shear wave. It is found that,

different waves travel with different frequencies. Hence in order to identify the shear wave, one should explicitly evaluate the frequency spectrum of the captured signal.

4.2.1 Digitizing the Time Axis

A continuous time analog signal $x_a(t)$ has to be converted into a sequence of discrete time signals, represented by a sequence of numbers x , denoted $x[n]$, with n being the n^{th} number in the sequence. Such a sequence is the result of periodic sampling of the continuous time analog signal $x_a(t)$,

$$x[n] = x_a(nT) \quad (4.3)$$

T is the sampling period, and $1/T$ the sampling rate or sampling frequency. For ultrasonic applications this is typically in the MHz range. The sampling frequency, $\Omega_s = (1/T)$, has to be greater than the bandwidth Ω_N of the signal being sampled. More precisely, according to the Nyquist Sampling Theorem, for a correct representation of a digitized signal, the sampling frequency Ω_s has to be at least twice as high as the bandwidth Ω_N :

$$\Omega_s = 2\pi/T > \Omega_N \quad (4.4)$$

Under-sampling, or sampling at rates less than the Nyquist requirement will cause "aliasing", which results in "shadow frequency images" of the original signal.

4.2.2 Digitizing Signal Amplitude

The A/D converter performs the initial amplitude discretization for the input analog ultrasonic signal prior to further conversion needed during processing by either a fixed or floating-point signal processor. This conversion process quantizes the signal amplitudes into a sequence of finite-precision samples. The number of amplitude quantization levels determines the precision or quantization error. This quantization error can be represented as an additional noise signal component.

4.2.3 Time –Frequency Analysis.

In many applications it is of interest to know the frequency content of a signal locally at a time. That is, the signal parameters (frequency content etc.) evolve over time. Such signals are called *non-stationary*. For a non-stationary signal, $x(t)$, the standard Fourier transform is not useful for analyzing the signal. Information, which is localized in time such as, spikes and high frequency bursts can not be easily detected from the Fourier transform. Time-localization can be achieved by first windowing the signal so as to cut off only a well localized slice of $x(t)$ and then taking its Fourier transform. This gives rise to the Short Time Fourier Transform, (STFT) or windowed Fourier Transform. The magnitude of the STFT is called the *spectrogram*.

4.2.4 Time and Frequency.

Fourier analysis is well known technique of signal processing, which breaks down the signal into constituent sinusoids of different frequencies. The *Fourier Transform* (FT) is a technique to transform time-domain signal $x(t)$ into frequency- domain signal $X(f)$. Mathematically the *Fourier Transform* is given by

$$X(f) = \int_{-\infty}^{\infty} x(t)e^{-jft} dt \quad (4.5)$$

and its inverse,

$$x(t) = \int_{-\infty}^{\infty} X(f)e^{jft} df \quad (4.6)$$

where, f is the frequency. In *Fourier Transform*, the main drawback is that the time information is hidden. When looking at a FT of a signal, it cannot be seen when the particular spectral components appear exactly in the signal.

4.2.5 Short-Time Fourier Transform (STFT)

Short-Time Fourier Transform (STFT) is a modification of the Fourier transform. STFT analyzes a small section of the signal at a time. This technique is known as *windowing* of a signal. Mathematically the STFT, of a signal $x(t)$, using a window function $h(t)$ is defined as follows.

$$STFT(f, s) = \int_{-\infty}^{\infty} x(t)h(t-s)e^{-j2\pi ft} dt \quad (4.7)$$

Where, $h(t)$ is the analysis filter or analysis window. The STFT represents a compromise between the time-domain and frequency-domain views of a signal. It provides information about frequency content in the window of the signal at the given time. However, this information is obtained with limited precision, and that precision is determined by the size of the window. The drawback is that once a particular size is chosen for the time window, that window is the same for all frequencies. Many signals require a more flexible approach, where the window size can vary to determine more accurately in either time-domain or frequency-domain.

4.2.6. Spectrogram

The Wigner distribution and the spectrogram are most often used for TF analysis due to their simplicity in theory and implementation. The Wigner distribution is a two-dimensional function describing the frequency content of signal as a function of time and possesses many advantageous properties. Among them:

1. Instantaneous frequency property which says that, as the time instant t , the mean instantaneous frequency of the $T_x(t, f)$ is equal to the energy possessed by the original signal.
2. Because the Wigner distribution satisfies both time and frequency marginal conditions, it can be shown, that energy contained in the $T_x(t, f)$ is equal to the energy possessed by the original signal.

The spectrogram represents the time-varying spectrum of a signal as it computes the frequency content of the signal in short intervals. Specially, it provides information on which frequencies are present in a signal and how those frequencies vary with time. The spectrogram is simply the squared magnitude of the short time FT, which divides the signal in to successive short time segments by the sliding window $h(t)$ and determines the local spectrum by means of FT of the segment. It is based on the assumption that the signal is stationary over the short duration of the segment.

The primary purpose of the window in the STFT is to limit the extent of the sequence to be transformed so that the spectral characteristics are reasonably stationary over the duration of the window. The spectrogram involves a compromise between time resolution and frequency resolution: a longer window provides less localization in time and more discrimination in frequency. If the window is too long, it fails to capture the most rapid variations of spectral content. If it is too short, it smears the time-frequency distribution in the frequency dimension without a commensurate improvement in detail in the time dimension. The more rapidly the spectral content changes, the shorter the window must be. The duration of the window affects the TF localization offered by the spectrogram in time and frequency. Furthermore, a trade-off exists between time and frequency localization because no window exists that is perfectly concentrated in both time and frequency domains due to the Uncertainty principle. Specifically, a longer analysis window yields poorer time resolution but better frequency localization; conversely, a shorter analysis window yields better time localization but poorer frequency localization.

4.3 CLOSURE

In this chapter the radiation pattern of laser ultrasonic sources is described. The theoretical directivity patterns for pressure wave and shear wave are drawn. The basics of signal processing as applicable to processing of ultrasonic signals are explained.

Chapter 5

RESULTS AND DISCUSSION

In this chapter the results achieved in this work are discussed. Firstly the directivity patterns of pressure wave in samples are presented followed by characterization of shear wave. After characterizing the shear wave, its time of arrival followed by the directivity pattern of shear wave is presented.

5.1 EXPERIMENTAL DETAILS

In the experimental arrangement using laser heterodyne detection, it is necessary that the probe laser beam has to be reflected from the surface under investigation. Because the carrier wave which carries the information is built up from the reflected light from the surface through constructive interference phenomenon. Better the reflected light, stronger the carrier wave. Under the circumstances if ultrasonic waves generated in the material is detected at the epicenter as shown in Fig 5.1, one can only detect the pressure wave displacements, as the shear wave displacements are transverse and cannot cause disturbance in the probe beam direction. However, if the ultrasonic signal is picked up at a point away from the epicenter (off-epicenter) as shown in Fig 5.2 with the probe beam continuing to be normal to the surface then, the heterodyne will be able to pick up the components of vibrational amplitudes of both pressure wave and shear (horizontal) wave.

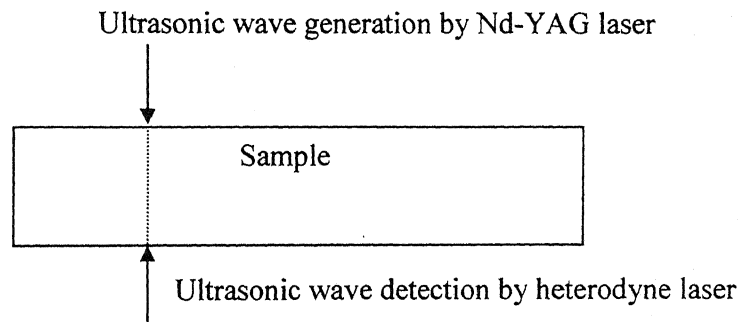


Fig 5.1 Epi-central measurement

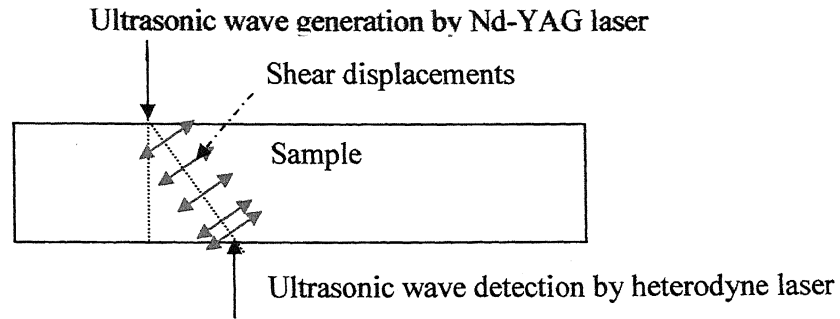


Fig 5.2 Off Epi-central measurement with shear displacements

keeping the above-mentioned limitations, experiments are designed on aluminum samples so as to identify and characterize the pressure and shear wave spectra. The experimentation was carried out on three different types of samples. That is on, semi-cylindrical, rectangular and stepped sample as shown in fig 5.3, fig 5.21 and fig 5.23 respectively. Semi-cylindrical samples are used for obtaining the directivity of pressure wave. Experiments on rectangular sample are carried out to characterize the shear waves in terms of frequency, while the experiment on stepped sample are conducted to obtain the directivity pattern of shear wave.

5.2 DIRECTIVITY PATTERN OF LASER SOURCE FOR PRESSURE WAVE

In order to obtain the directivity pattern of laser source for pressure wave, ultrasonic waves are recorded on semi cylindrical samples of different radii at different angles from the source. The samples of radii 20mm, 25mm and 30mm are used. Semi-cylindrical samples have been chosen so that the distance traveled is same for all measurements. The heterodyne probe is always adjusted normal to the surface at the point of measurement so that it catches the magnitude of pressure wave without being affected by shear wave displacements.

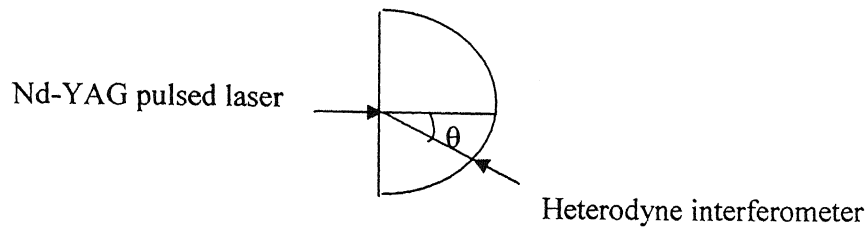


Fig 5.3 semi cylindrical sample with pulsed laser and heterodyne interferometer

5.2.1 Sample of 25mm radius

The experiments are carried out on a 25mm semi-cylindrical aluminum sample at various angles. Figs 5.4 to 5.9 show a few signals obtained experimentally on 25 mm radius sample. In all these, due to its higher velocity compared to other, the pressure wave is expected to arrive first i.e. first arrival. Hence the first significant displacement after the trigger point is taken as the amplitude corresponding to pressure wave. The time of arrival of first peak turned out to be around 4 microseconds, which agrees with the value available in literature [3].

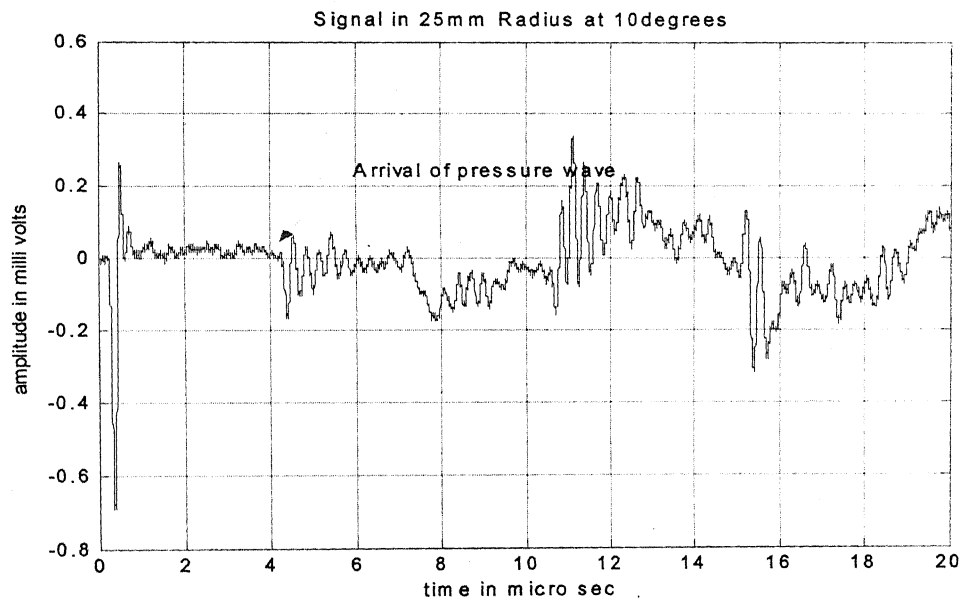


Fig 5.4 Signal collected in 25mm radius sample at 10^0 from the epicenter

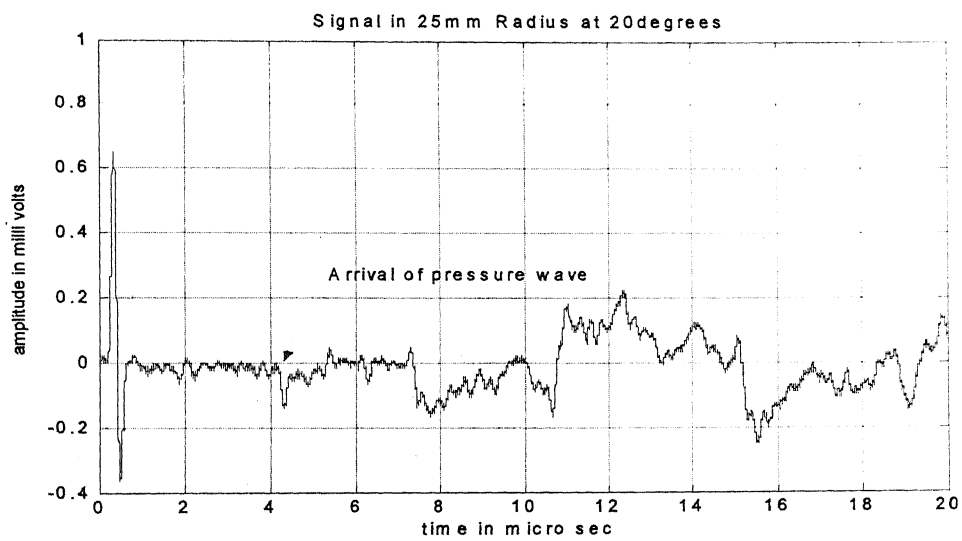


Fig 5.5 Signal collected in 25mm radius sample at 20° from the epicenter

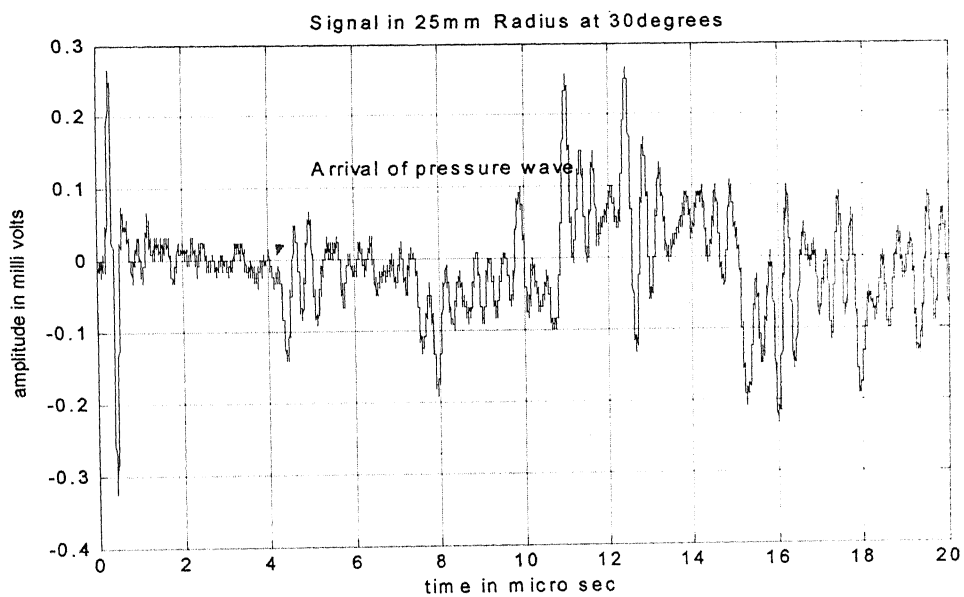


Fig 5.6 Signal collected in 25mm radius sample at 30° from the epicenter

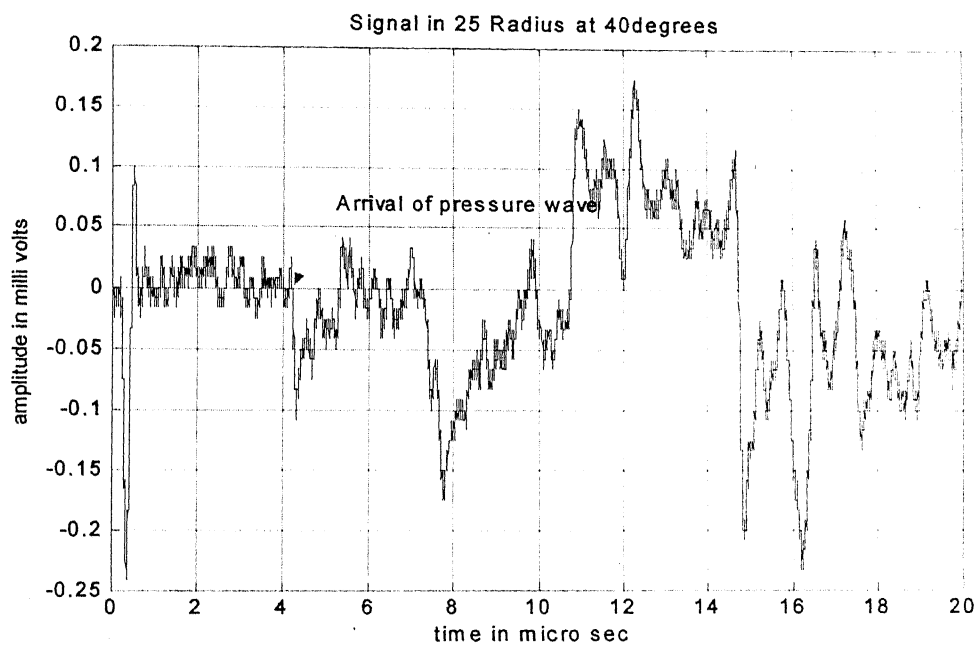


Fig 5.7 Signal collected in 25mm radius sample at 40° from the epicenter

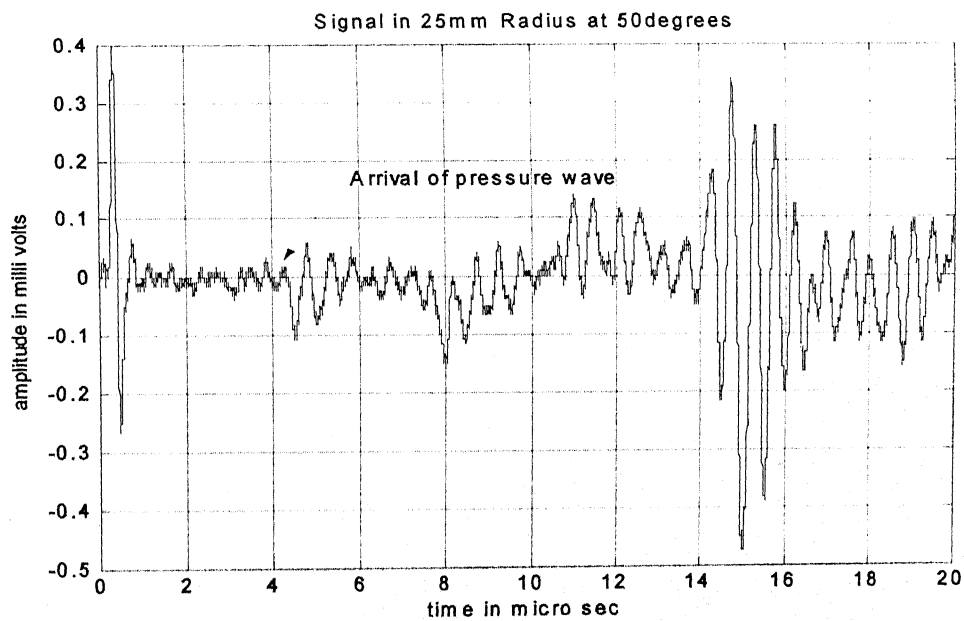


Fig 5.8 Signal collected in 25mm radius sample at 50° from the epicenter

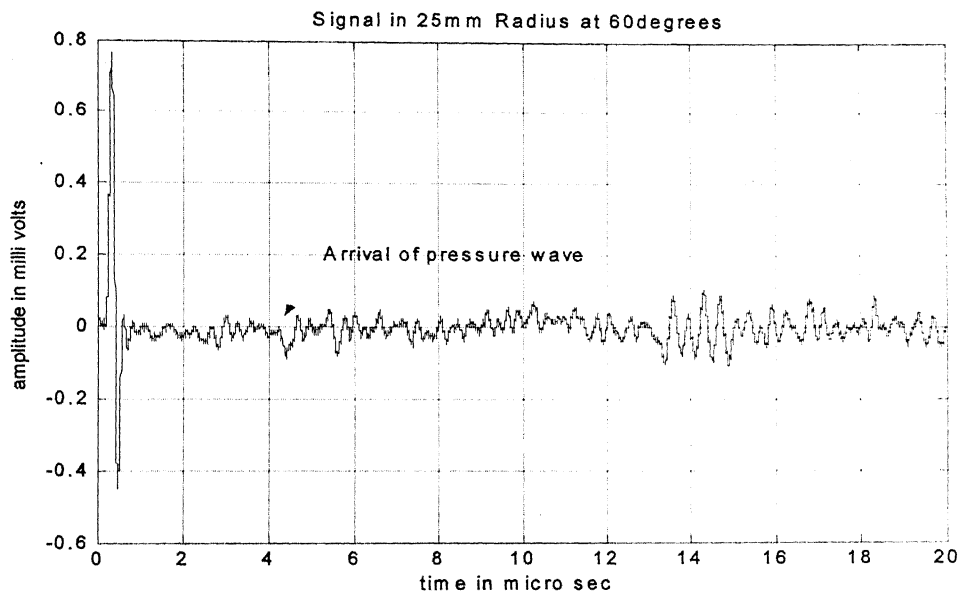


Fig 5.9 Signal collected in 25mm radius sample at 60° from the epicenter

From the above signals, one can clearly see that the amplitude of pressure wave keeps decreasing with the increase in angle from the epicenter. This is in accordance with the literature [1]. As discussed in section 4.2, the directivity pattern has been drawn measuring the amplitudes of pressure wave at various angles, which is shown in Fig 5.10.

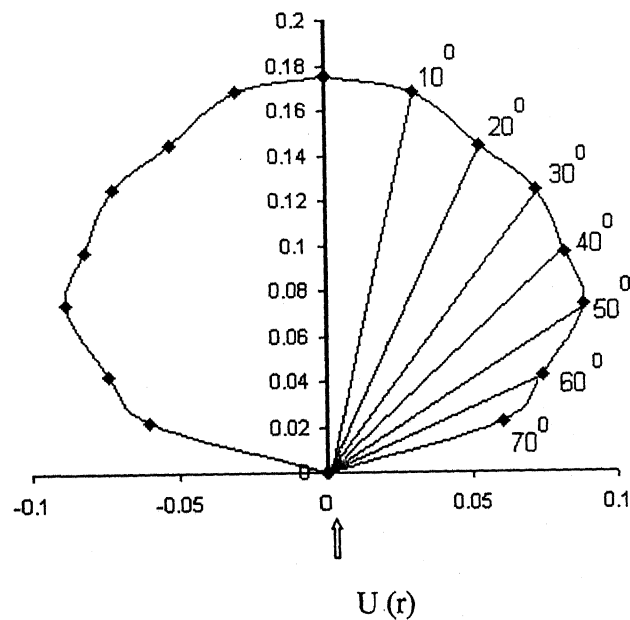


Fig 5.10 Experimentally obtained directivity of pressure wave in 25mm radius

5.2.2 Sample of 20mm radius

In order to know the effect of distance on the pressure wave attenuation and the power of laser source on the directivity pattern in ablation regime, the experiments are conducted on aluminum of 20mm radius and 40mm radius samples. Signals are obtained from 0° to 70° in steps of 10° starting at epicenter. The power of laser is changed to higher value but still in the ablation regime. A few signals obtained experimentally in 20mm radius are shown below in Fig 5.11 to Fig 5.13.

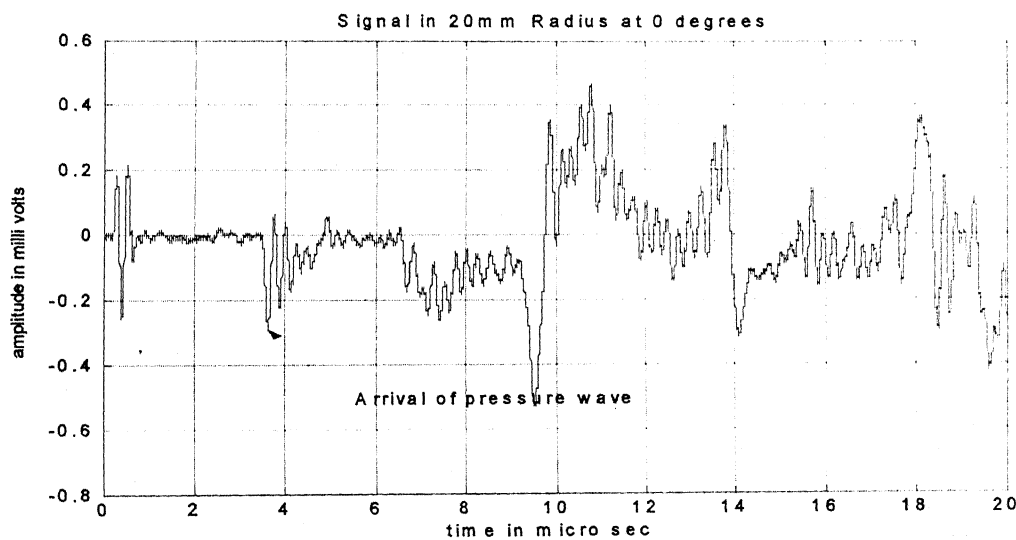


Fig 5.11 Signal collected in 20mm radius sample at 0° (epicenter)

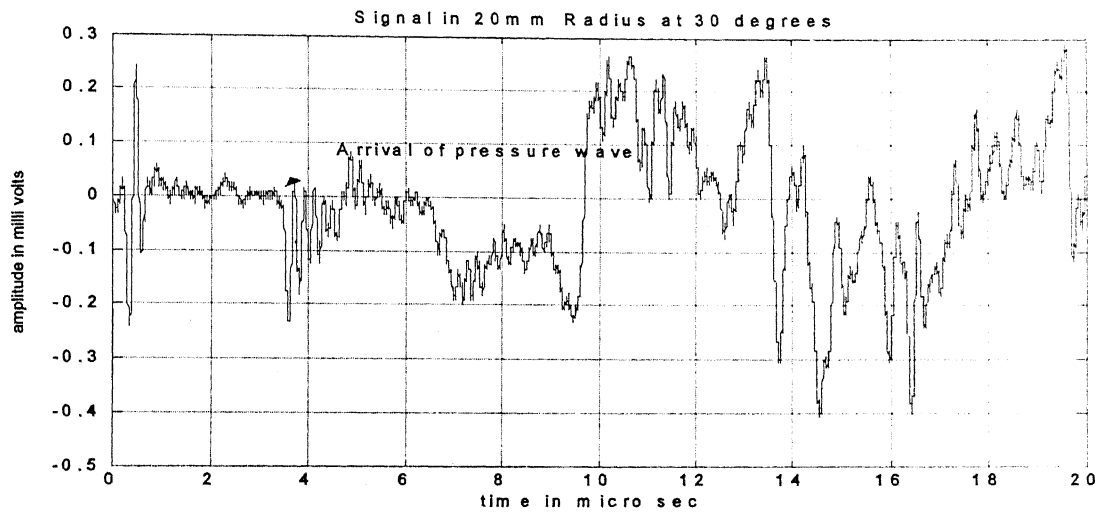


Fig 5.12 Signal collected in 20mm radius sample at 30° from the epicenter

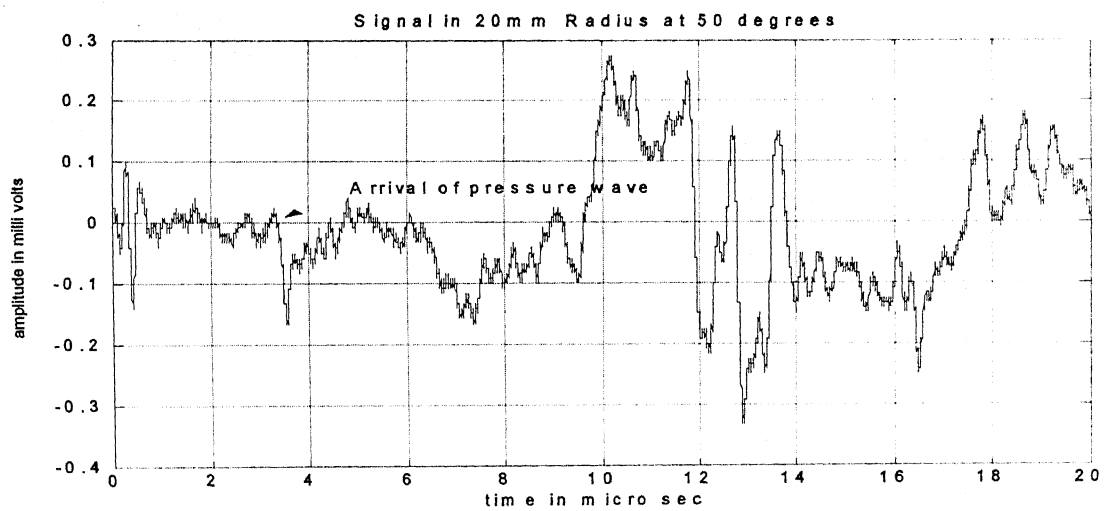


Fig 5.13 Signal collected in 20mm radius sample at 50° from the epicenter

From the above signals one can see that the pressure wave time of flight for 20mm distance traveled is approximately 3.2 microseconds. The directivity pattern as obtained by measuring the amplitudes of pressure wave signals is shown in fig 5.14.

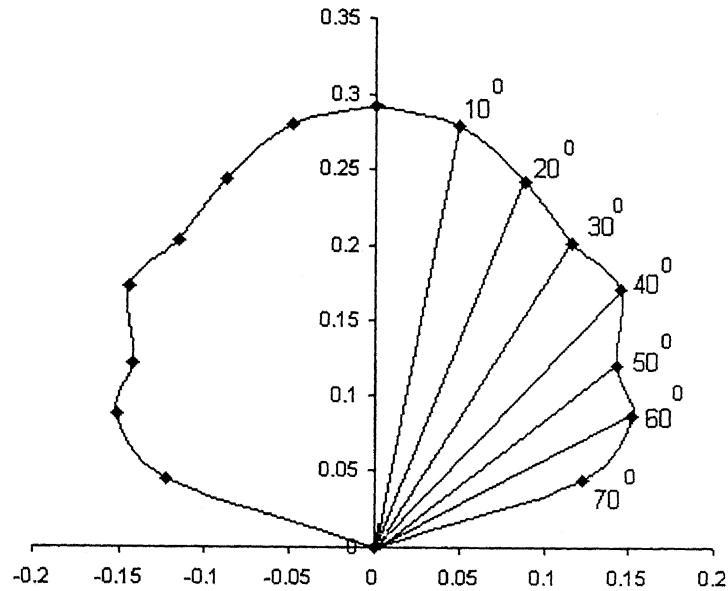


Fig 5.14 Directivity of pressure wave at 20mm radius

5.2.3 Sample of 40mm radius

With the same power that is used for 20mm radius sample, experiments are conducted on 40mm radius aluminum sample to correlate directivity pattern dependency with distance traveled. Some of the signals in 40mm radius are shown in fig 5.15 to fig 5. 17.

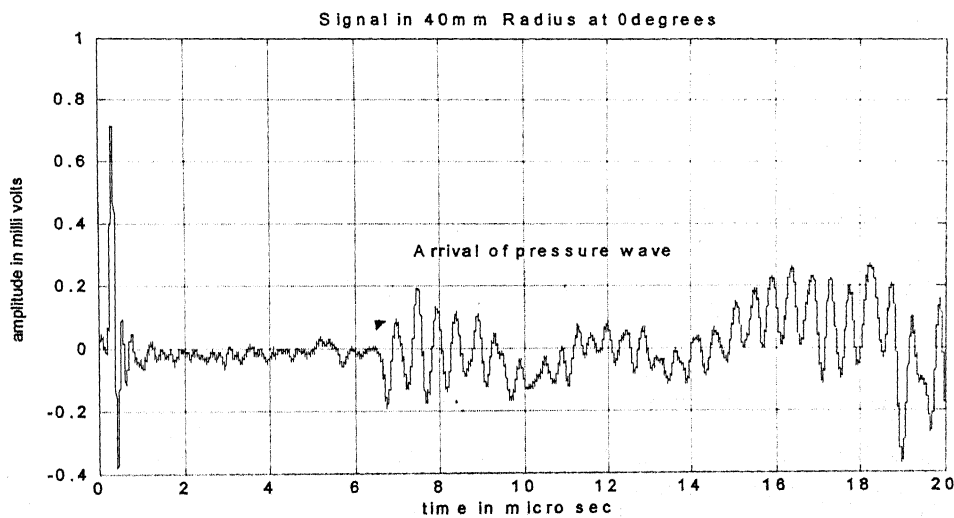


Fig 5.15 Signal collected in 40mm radius sample at 0° (epicenter)

मुद्रणोत्तम काशीनाथ केलकर पुस्तकालय
भारतीय प्रौद्योगिकी संस्थान कानपुर
प्रवाहित क्र० A... 149261

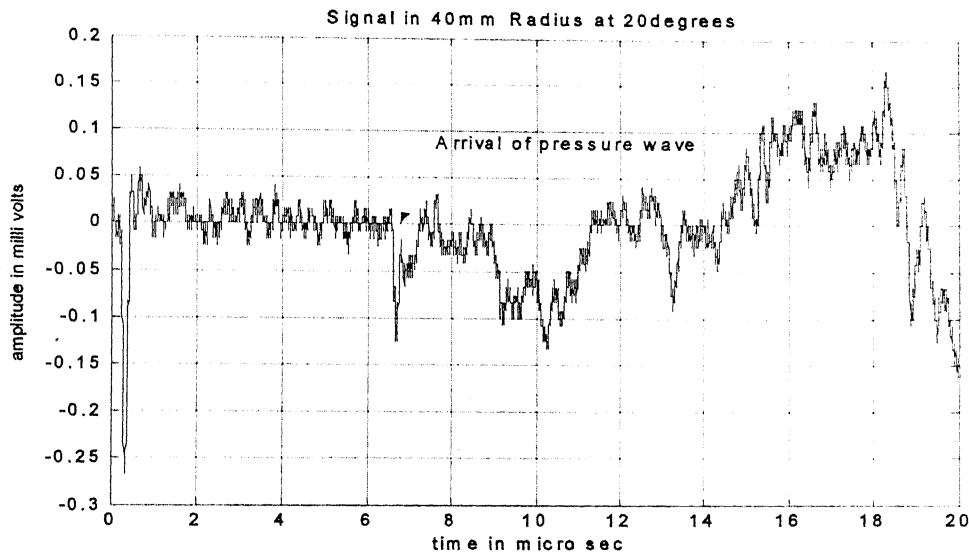


Fig 5.16 Signal collected in 40mm radius sample at 20° from the epicenter

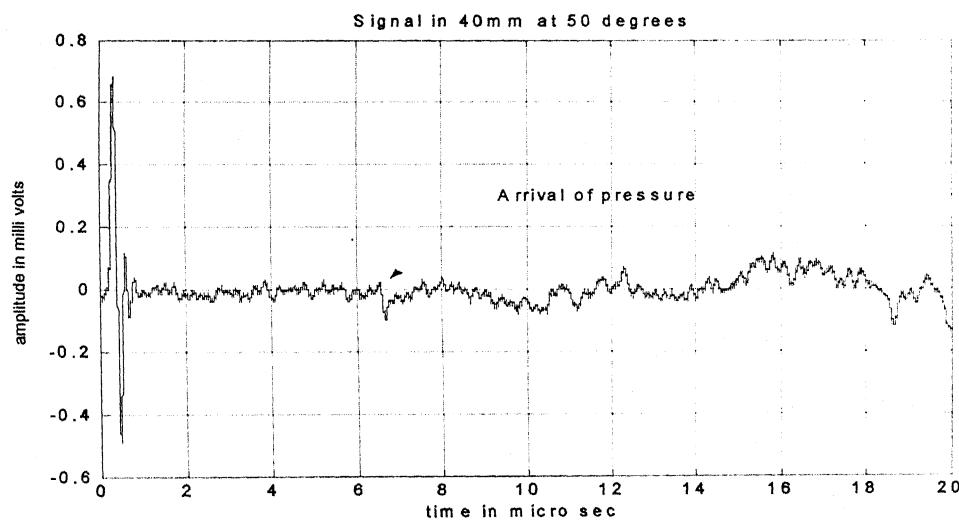


Fig 5.17 Signal collected in 40mm radius sample at 50° from the epicenter

The directivity pattern obtained from the above signals is shown below in fig 5.18. From the obtained signals and the directivity pattern it can be inferred that in ablation regime, the amplitudes of the pressure waves are in direct proportion with distance travelled and is also dependent of the incident laser energy [7].

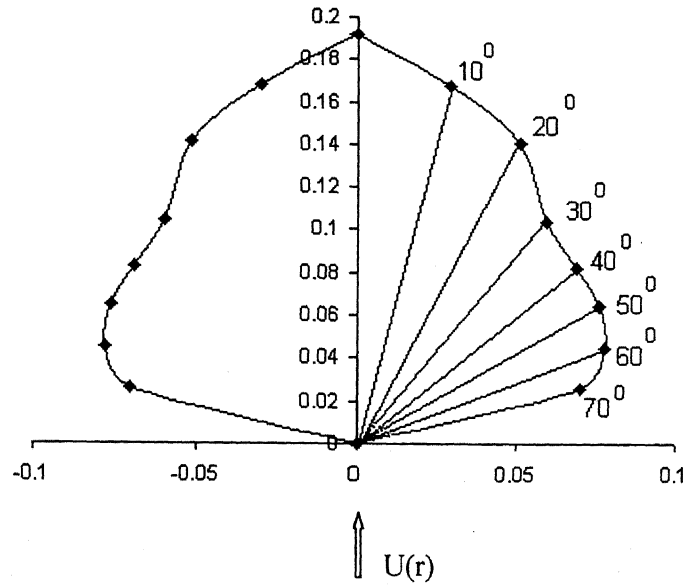


Fig 5.18 experimentally obtained Directivity of pressure wave in 40mm radius

5.3 SHEAR WAVE IDENTIFICATION

The recognition of shear wave arrival (corresponding to shear displacement) is a difficult task as it gets mixed up with the P-wave, which comes earlier. Arnold et al [3] showed a method of recording the displacements corresponding to shear wave by a specially designed interferometer system. In order to find the shear wave time of flight with the present experimental setup, i.e., making use of heterodyne interferometer for detection one should make use of some characteristic property of the shear wave. In order to characterize shear waves, ultrasonic waves are recorded on a rectangular sample of 25mm thickness in various directions as shown in fig 5.21. As discussed in Chapter 4, extensive signal processing has been carried out. The experimentally obtained signals from 0° , 70° in steps of 10° are processed for getting information of frequency contents of the signals. Theoretically, the shear wave is expected to be predominant at around 40° .

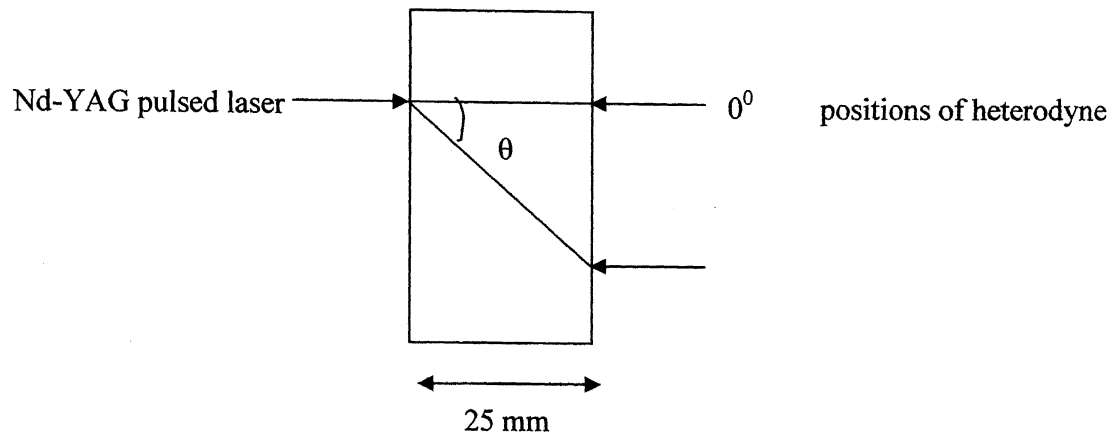


Fig 5.19 Rectangular sample

For comparative study the FFTs of two signals obtained at 0° (epicenter) and 45° from the epicenter are plotted in the same figure (Fig 5.20). FFTs obtained are analyzed and compared with one another in the time-frequency characteristics with the variation of angle from the epicenter.

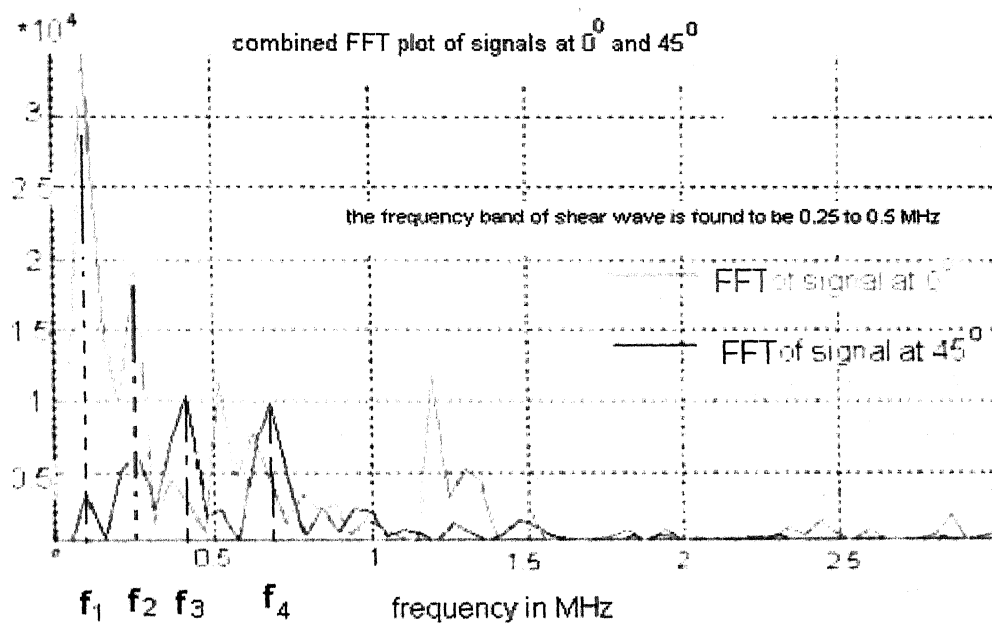


Fig 5.20 Combined FFT of signals at 0° and at 45°

The wave at 0° is purely due to pressure wave whereas the wave at 45° comprises of contributions from both pressure wave and shear wave. A comparison of various peaks of the two curves leads one to draw the following conclusions: From FFT curve obtained for 45° wave, it is evident that the component at f_1 - frequency is purely due to pressure wave. And component at f_2 is a superposition of pressure wave and shear wave, whereas components at f_3 and f_4 are due to shear wave arrival only, because if there is no shear wave arrival at 45° , the FFT would follow the same pattern as that of 0° (i.e. as a peak at f_1 and f_2). But at frequencies f_3 and f_4 this trend was not followed. This will lead one to draw the conclusion that because of shear wave arrival, signal at few other frequencies start becoming significant. It can be deduced that signal components at f_2 , f_3 and f_4 are due to shear wave. Similar conclusions were drawn from the signals obtained at other angles. From these observations the shear wave frequencies are expected to lie within the band of 0.25 to 0.75 MHz. It was found for all the signals in aluminum that this band correspond to shear wave. using the above frequency band, which signify the shear wave, the time of flight and the directivity pattern of shear wave is evaluated. This is discussed in detail in the following sections.

5.4 SHEAR WAVETIME OF ARRIVAL AND ITS DIRECTIVITY IN A LENGTH OF 25 MM

After characterizing the shear waves with the characteristic frequency band, an effort has been made to find out the time of its arrival at a distance of 25mm. To achieve this experiments are conducted on a stepped sample as shown in fig 5.21. The distance between the transmitter (Nd_YAG pulsed laser) and receiver (heterodyne interferometer) is maintained constant at 25mm at various angles from the epicenter as shown in fig 5.21. The stepped sample as shown in figure (fig 5.21) has been chosen to ensure that the attenuation of signal in all directions is same without affecting the component of shear wave being measured by the laser heterodyne interferometer. This has been achieved by ensuring that the loci of the mid point (the point of measurement) of each step lie on a circular arc of 25mm radius. To find out the time of flight an extensive time-frequency analysis of the signals has been carried out. In the time-frequency domain the frequency

band corresponding to shear wave arrival is examined. Time-frequency analysis has been carried out using MATLAB and SIGVIEW signal processing software.

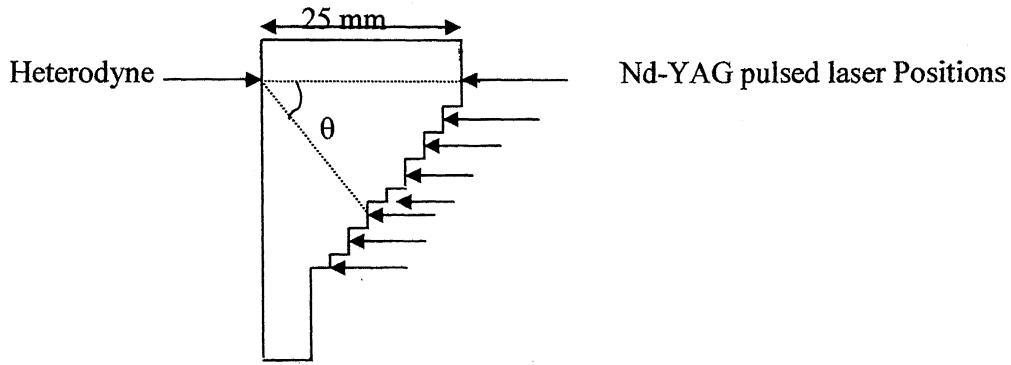


Fig 5.21 Stepped sample

The signals are collected from 0° to 70° in steps of 10° . The combined FFT of all these signals is shown in fig 5.22.

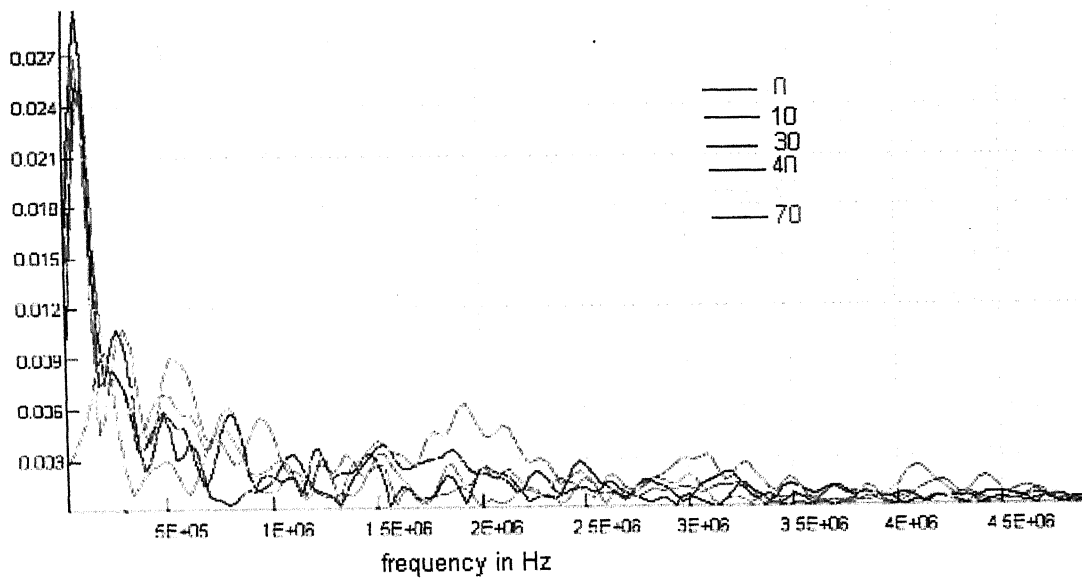


Fig 5.22 FFT plots of the signals collected at various angles

5.4.1 Time of arrival of shear wave

In order to find out the time of arrival of shear wave, time frequency analysis has been carried out. As the frequency band of interest that characterizes shear waves in aluminum is 0.25 to 0.75 MHz, the window size for analysis has been chosen in such a way that this band of frequencies are not missed out in Time-frequency plots. Since the sampling frequency is 500 MHz, Size of the window has been taken to be 2048 with an overlap of 2046 points. Time-frequency plots for the experimentally obtained signals on stepped sample are shown in Fig 5.23(a) to Fig 5.23(e).

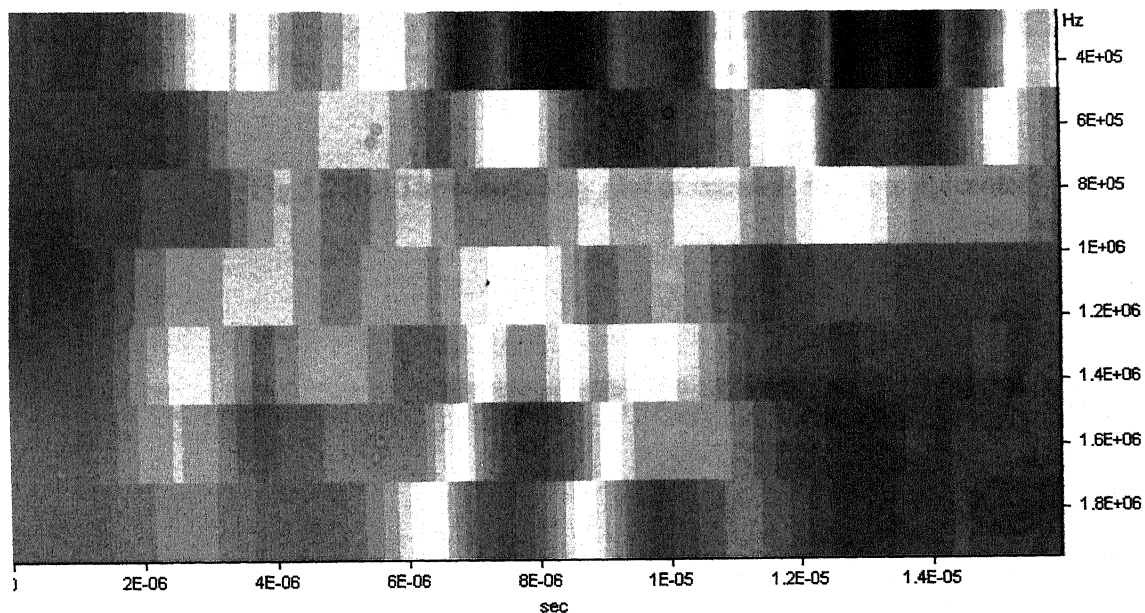


Fig 5.23(a) Time-frequency plot of signal at 30^0 from epicenter.

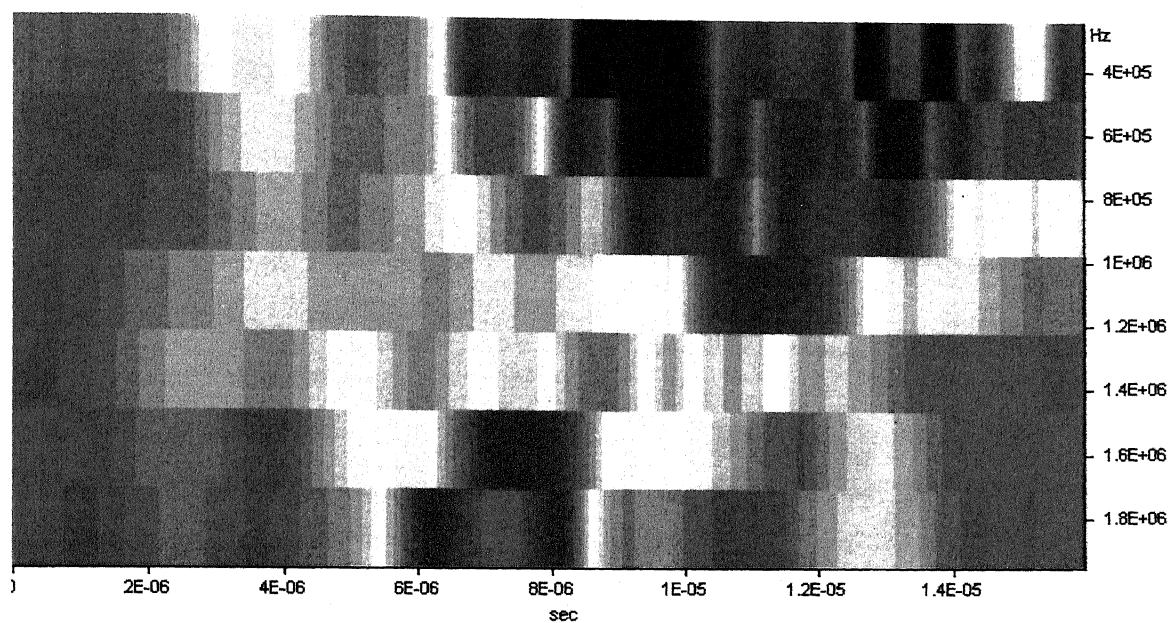


Fig 5.23(b) Time-frequency plot of signal at 40° from epicenter

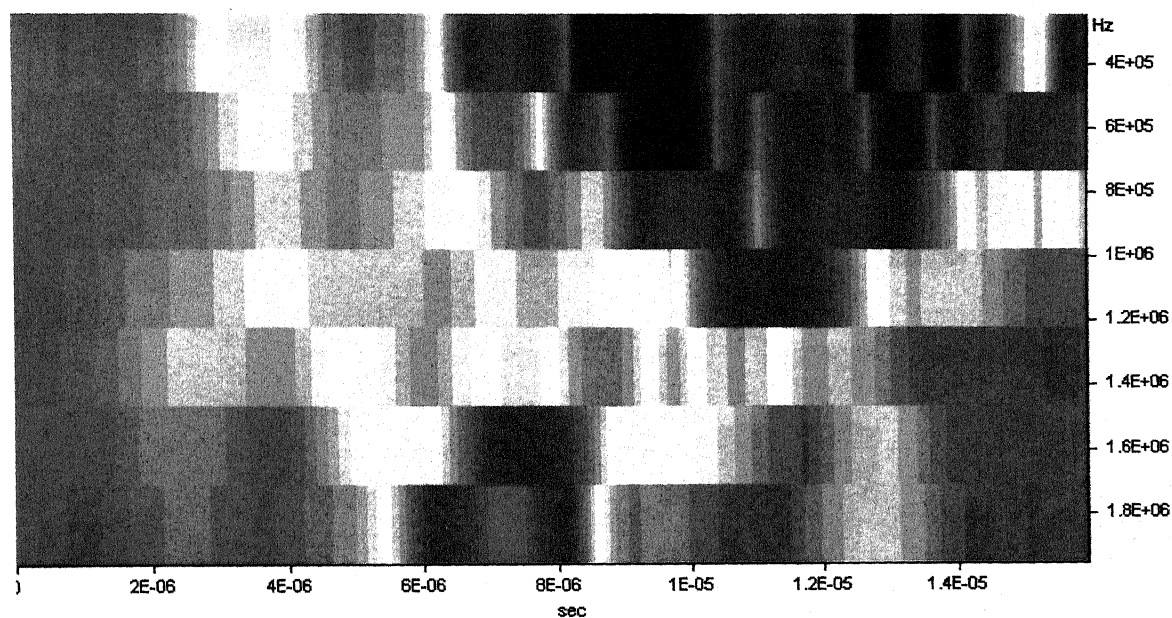


Fig 5.23(c) Time-frequency plot of signal at 50° from epicenter

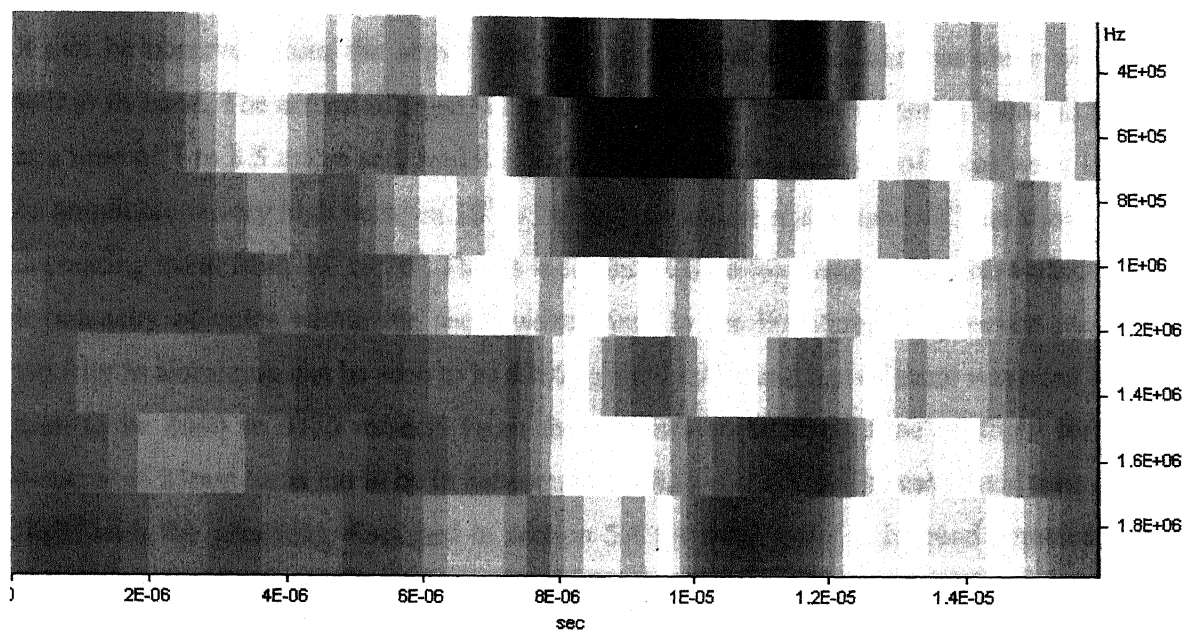


Fig 5.23(d) Time-frequency plot of signal at 60° from epicenter

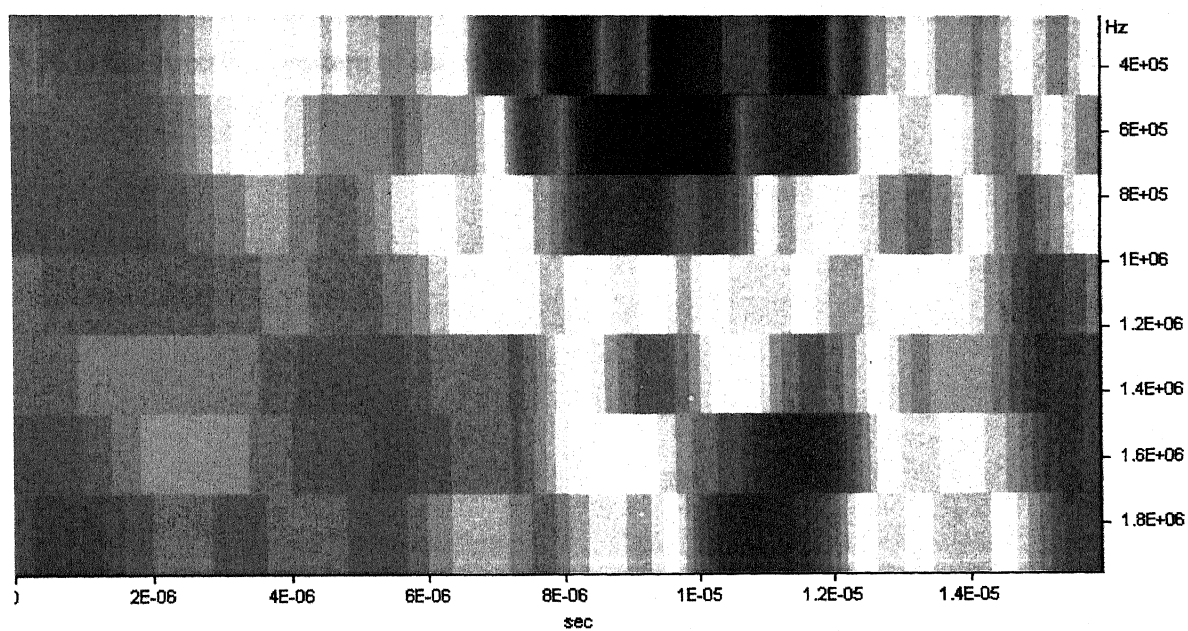


Fig 5.23(e) Time-frequency plot of signal at 70° from epicenter

It can be observed from the above plots, the first arrival can be taken as shear wave within its band. The arrival of shear wave with the known frequency band is found to be at a time of 7 to 8.5 micro sec. And it is clearly seen that the intensity of shear wave i.e. its amplitude is very high between 10^0 to 70^0 and is maximum at around 40^0 and shows a decreasing trend from 40^0 to 70^0 . This is indicated in time-frequency plots with variation in intensity of color within the shear wave band. In the literature, the pressure wave velocity in aluminum can be seen to be 6250 to 6500 m/sec and that of shear wave can be seen to be 3040 to 3130 m/sec. From these values shear wave, time of flight for a distance of 25mm turns out to be in between 7.8 to 8.22 micro sec. The calculated time of flight with the reasoning discussed in section 5.4 for shear wave is in good agreement with the data available in literature.

5.4.2 Shear wave directivity pattern

Having calculated the time of arrival of shear wave, an attempt has been made to determine the displacement corresponding to shear wave i.e. shear wave component in the experimentally obtained signals. At calculated times of flights, amplitude values for those frequencies were chosen for drawing the directivity pattern. Shown below in Fig 5.26 is the directivity pattern of shear wave.

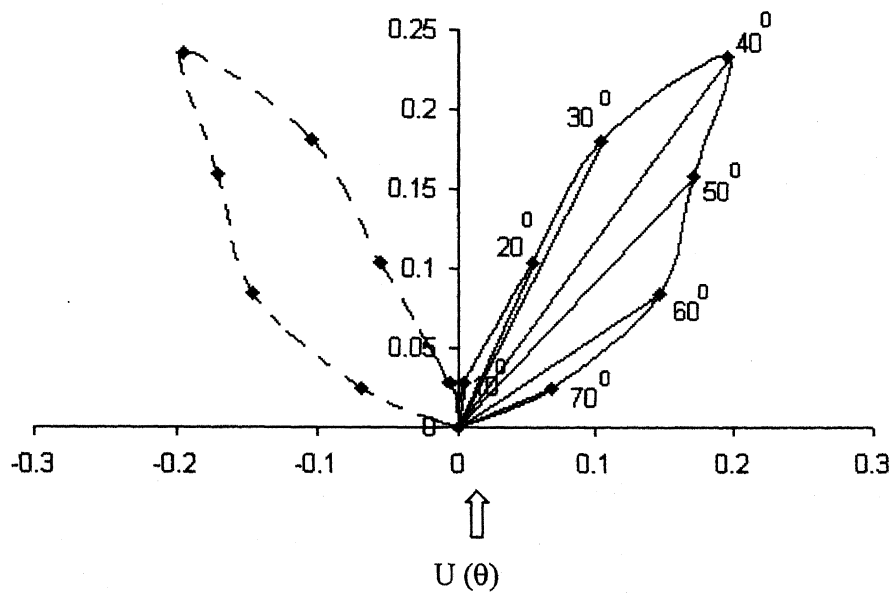


Fig 5.26 Directivity of shear wave

Experimentally obtained directivity pattern of laser source for shear wave shown above is well in agreement with the theoretical pattern as discussed in section 4.2.1 at all the angles except at an angle 30° . Here the amplitude of shear wave instead of showing lower value when compared to the amplitudes at either 10° or 20° , showed an increasing value. From the above discussion one can come to the conclusion that the identification of shear waves based on the frequency spectrum is a reliable method with the available experimental set up.

Chapter 6

CONCLUSIONS AND SCOPE FOR FUTURE WORK

6.1 Conclusions

In the present study, the Laser Based Ultrasonic (LBU) system has been used to characterize both pressure and shear waves. Extensive experimental work has been carried out on aluminum. Experimentally obtained signals are processed to get time-frequency information. Based on the results obtained, the following conclusions are drawn:

1. The narrow pulses of laser used for generation of ultrasound leads to precise measurements of time-of-flight and therefore of component thickness or sound velocity.
2. Time-frequency analysis is shown to be an effective method that can be used to identify and characterize pressure and shear waves in metals.
3. The radiation pattern of laser source for pressure wave is drawn using the first arrival concept. The obtained directivity pattern seemed to be following the theoretical pattern. The same procedure can be adopted for other metals to obtain directivity pattern.
4. In aluminum, the frequency band corresponding to shear wave arrival is found be 0.25-0.75 MHz.
5. The radiation pattern of shear wave has been drawn, by knowing its characteristic frequency band.

6.2 Scope for future work

1. The time of flight studies can be carried out on various materials i.e. isotropic and anisotropic to obtain information of pressure and shear waves so as to reconstruct the defects in these materials applying tomographic reconstruction methods.

2. Time-frequency analysis can be used for characterizing the pressure and shear waves in composite materials, which is a challenging area for Non-destructive testing.

Bibliography

1. Scruby C.B. and Drain L.E. "*Laser Ultrasonics: Techniques and Applications*", Adam Hilger Bristol, Philadelphia, New York, 1990.
2. Krautkramer J. and Krautkramer H. "*Ultrasonic Testing of Materials*", 4th edition Springer-Verlag, New York, 1990
3. S.Y.Zhang., M.Paul., S.Fassbender., U.Schleichert., and W.Arnold, "*Experimental Study of Laser-Generated Shear Waves Using Interferometry*", Res Nondestructive Evaluation, 1990, Vol.2, pp. 143-155.
4. Pengzhi Zhang., C.F.Ying and Jianzhong Shen, "*Directivity patterns of laser thermoelastically generated ultrasound in metal with consideration of thermal conductivity*", Ultrasonics, 1996, Vol. 35, pp 233-240.
5. S.Fassbender., B.Hoffman., and W.Arnold, "*Efficient Generation of Acoustic Pressure Waves by Short Laser Pulses*", Material Science and Engineering , 1989, A122, pp.37-41.
6. Osamu Matsuda., and Oliver B.Wright, "*Theory of Detection Of Shear Strain Pulses with Laser Picosecond Acoustics*", Analytical Sciences, 2001, Vol.17, pp s216-s218, The Japan Society for Analytical Chemistry.
7. C.B.Scruby., R.J.Dewhurst., D.A.Hutchins., and S.B.Palmer, "*Quantitative studies of thermally generated elastic waves in laser-irradiated metals*", J. Applied Physics, 1980, Vol.51(12), pp 6210-6216.
8. R.J.Dewhurst., D.A.Hutchins., S.B.Palmer., and C.B.Scruby, "*Quantitative Measurement of laser-generated acoustic waveforms*", J.Applied Physics, 1982, Vol.53(6), pp 4064-4071.
9. A.Hoffmann., and W.Arnold, "*Modelling of the ablation source in laser-ultrasonics*", Review of Progress in Quantitative Nondestructive Evaluation, 2000, pp 279-286.
10. J.D.Aussel and J.P.Monchalin, "*Measurement of ultrasound attenuation by laser ultrasonics*", J.Applied Physics, 1989, Vol. 65(8), pp 2918-2921.
11. Jin Huang., Yasuaki Nagata., Sridhar Krishnaswamy, and Jan D.Achenbach, "*Laser Based Ultrasonics for Flaw Detection*", Ultrasonic Symposium, 1994, pp 1205-1209.

12. Christophe Barriere, and Daniel Royer, “ *Optical Measurement of Large Transient Mechanical Displacements*”, Applied Physics Letters, 2001, Vol.79, Number 5.
13. W.Arnold., B.Betz., and B.Hoffmann, “ *Efficient generation of surface acoustic waves by thermoelasticity*”, Applied Physics Letters , 1985, Vol.47(7), pp 672-674.
14. Wu Yaping., Shi Dufang, and He Yulong, “ *Study of the directivity of laser generated ultrasound in solids*”, J. Applied Physics, 1988, Vol.83(3), pp 1207-1212
15. A.E.Lord, J. Acoustic Society of America, 1966, Vol.39, pp 650.
16. L.R.F.Rose, J.Acoustic Society of America, 1984, Vol. 75, pp 723.
17. J.A.Cooper, Ph.D thesis, University of Hull, 1985.
18. C.B.Scruby., R.J.Dewhutchins., and S.B.Palmer, “Research Techniques in Nondestructive Testing(Academic , New York,1981)”.
19. P.A.Doyle, J.Physics, 1986,Vol.D19, pp 1613.
20. F.A.McDonald, “ Applied Physics Letters”, 1990, Vol.56, pp 1613.
21. L.Wu.J.C.Cheng., and S.Y.Zhang, “ J.Physics”, 1995, Vol. D28, pp 957.
22. Zeljko Andreic, “ *Time-Integrated Photographic Study of Laser Ablation at Large Impact Angles*”, FIZIKA, 1998, Vol. A7, pp 91-96.
23. J.D.Aussel and J.P.Monchalain, “ *Precision Laser-Ultrasonic Velocity Measurement and Elastic Constant Determination*”, Ultrasonics, 1989, Vol.27,pp 165-177.
24. Moushumi Zaman., Antonia Papandreou-Suppappola and Andreas Spanias, “ *Advanced Concepts in Time-Frequency signal Processing Made Simple*”, 33rd ASEE/IEEE Frontiers in Education Conference”, November 2003.
25. Ljubisa Stankovic., Tatiana Alieve and Martin J.Bastiaans , “ *Time-frequency signal analysis based on the windowed fractional Fourier transform*” , Signal processing, 2003, Vol. 83, pp 2459-2468.
26. Zbigniew Leonowicz., Tadeusz and Tomasz Sikorski , “ *Time-Frequency analysis of three phase signals Using Wigner Distribution*”, IV International Workshop “ *Computational Problems of Electrical Engineering*”, 2002, pp 81-84.

27. Datta D. "*A Methodology in Ultrasonic NDE for identification and reconstruction of defects in fiber composites*", *Ph.D. Thesis*, September 1995, Department of Mechanical Engineering, Indian Institute of Technology, Kanpur.
28. Sarin P.S. "*Development of laser-based ultrasonic Non-destructive testing*", *M.Tech. Thesis*, January 2002, Department of Mechanical Engineering, Indian Institute of Technology, Kanpur.
29. Daliraju G. "*Experimental characterization of laser-based ultrasonic system*", *M.Tech. Thesis*, February 2002, Department of Mechanical Engineering, Indian Institute of Technology, Kanpur.
30. Ramakrishna P. "*Ultrasonic Tomographic Reconstruction Of Defects In Composites with Ray Bending Consideration*", *M.Tech. Thesis*, April 2003, Department of Mechanical Engineering, Indian Institute of Technology, Kanpur.
31. Monchalain J.P., Neron C., Bussiere J.F. "*Laser-ultrasonics: from the laboratory to shop floor*", <http://www.ultraoptec.com/>

Appendix A

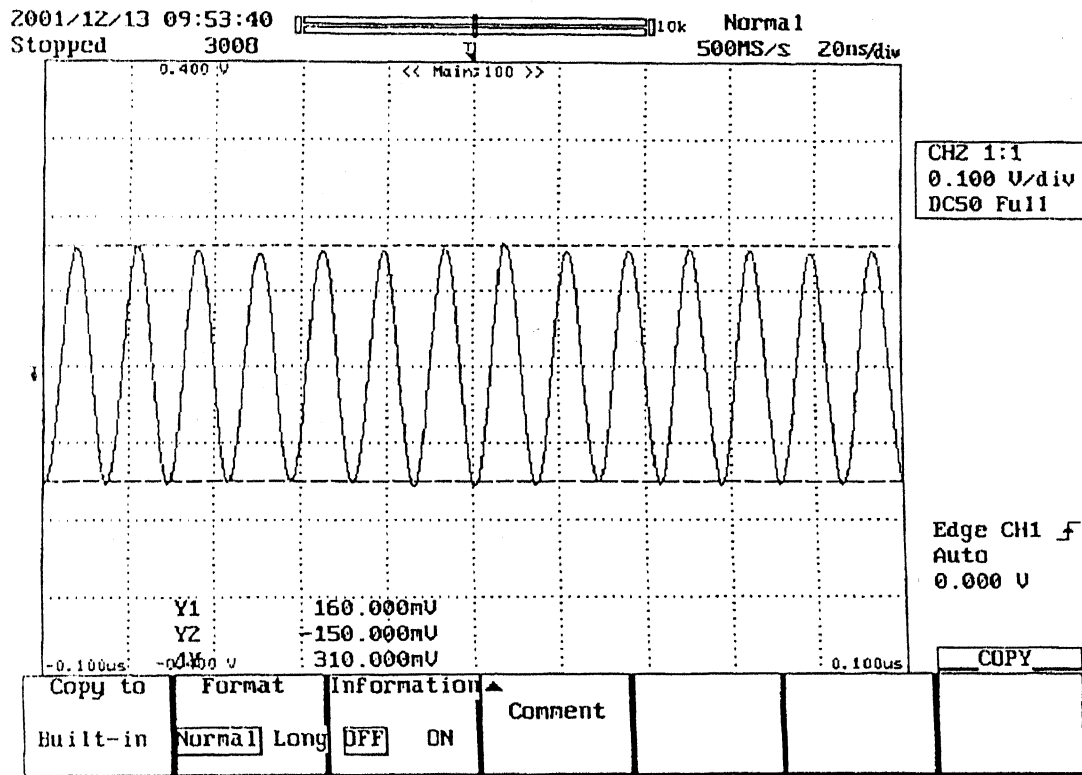
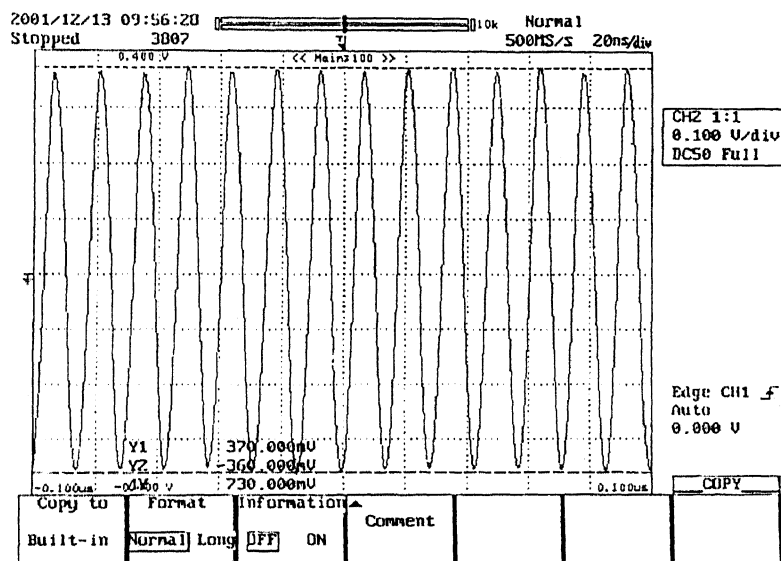
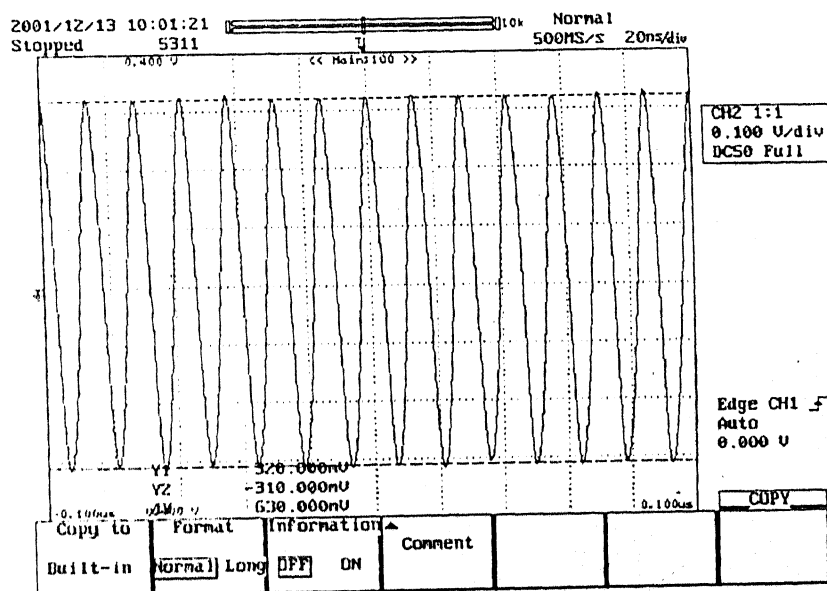


Photo Detector output measured without going through the Signal Processor.

Appendix B



**Output taken through the Signal Processor with the Automatic Gain Control
switched ON**



**Output taken through the Signal Processor with the Automatic Gain Control
switched ON after making adjustments available in the Signal-Processing Unit in
order to set it to 630mv**